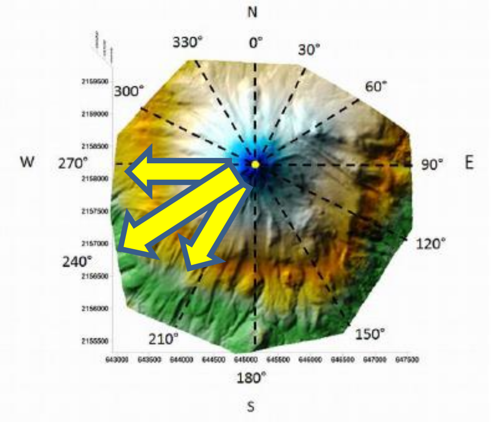

Modelado de estabilidad de taludes en el sistema solar: desde Marte, Luna y Ceres hasta volcanes y micro-taludes

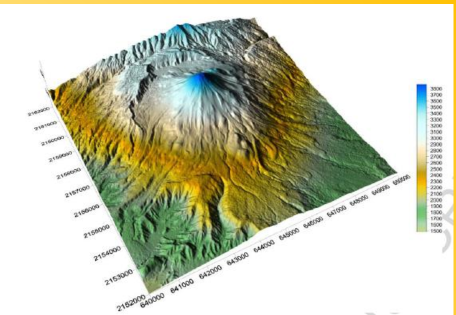

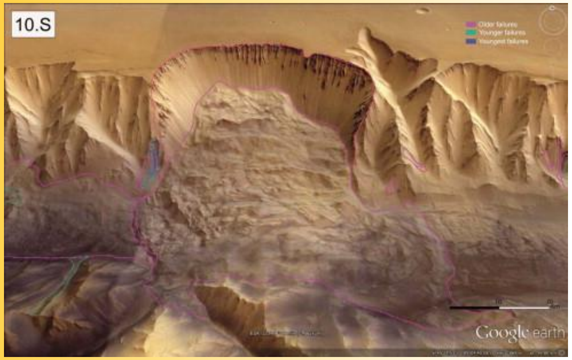

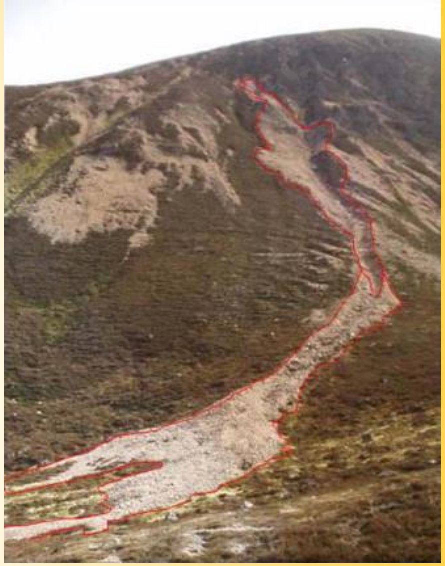

Lorenzo Borselli

Instituto de Geología

Universidad Autónoma de San Luis Potosí

Av. M. Nava No 5, Zona Universitaria,

San Luis Potosí, 78240, Mexico

lborselli@gmail.com

http://www.lorenzo-borselli.eu

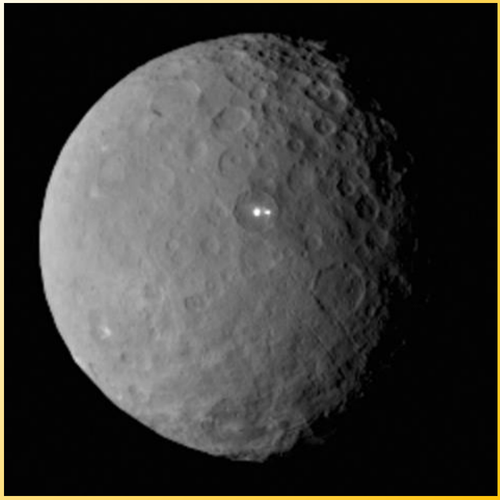

Campus de Geociencias UNAM, Queretaro -13-04-2016

Los fenómenos de deslizamiento, y otros inducidos por la gravedad, disparados por varios factores naturales o antrópicos, son un elemento extremamente importante en El proceso de evolución geomorfológica de cualquier cuerpo celeste de tipo terrestre.

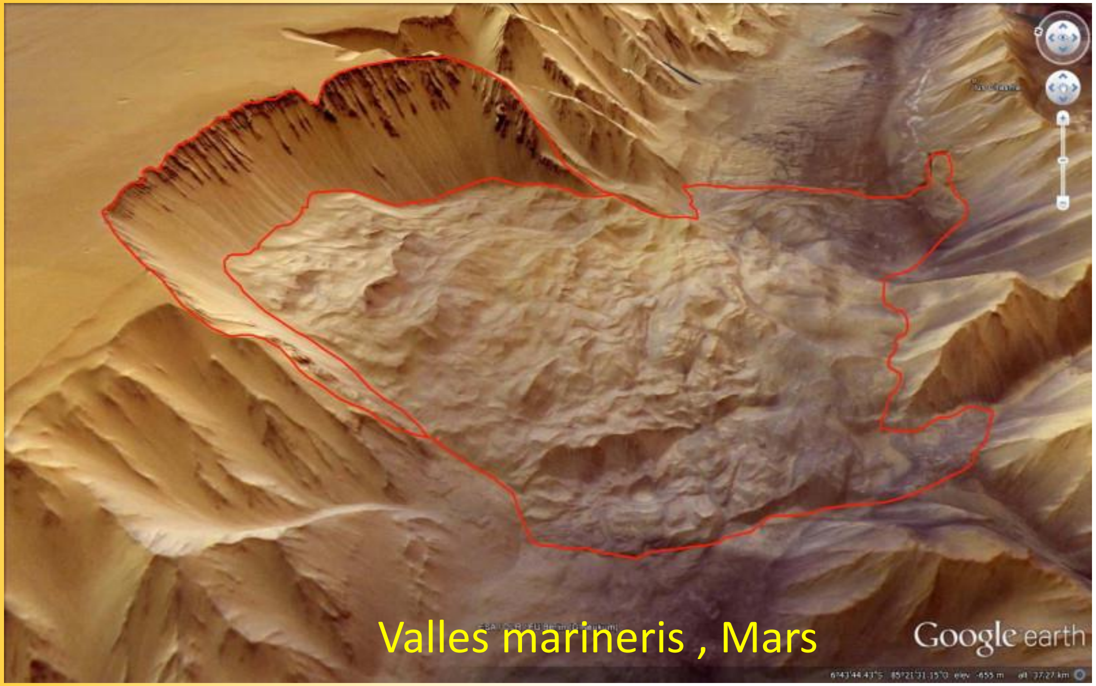

Los estudio geomorfológico, geológicos y geotécnicos que han sido desarrollado en la Tierra han sido aplicados, desde unas décadas, también en otros cuerpos planetarios del sistema solar.

Haciendo esto se ha descubierto muchas similitudes y algunos herramienta desarrollados en la tierra han resultados efectivos también para comprender los proceso en otros planetas.

En el Planeta Marte..

Masa	$6{,}4185 \times 10^{23}$ kg
Volumen	$1{,}6318 \times 10^{11}$ km^3
Densidad	3,9335 g/cm^3
Área de superficie	144 798 500 km^2
Diámetro	6794,4 km
Gravedad	3,711 m/s^2
Velocidad de escape	5,027 km/s
Periodo de rotación	24,6229 horas
Inclinación axial	25,19°

Gravedad 1/3 de la terrestre

https://es.wikipedia.org/wiki/Marte_(planeta)

Los proceso de inestabilidad son hoy en dia, y han sido, un importante factor de la evolución de la superficie del planeta.

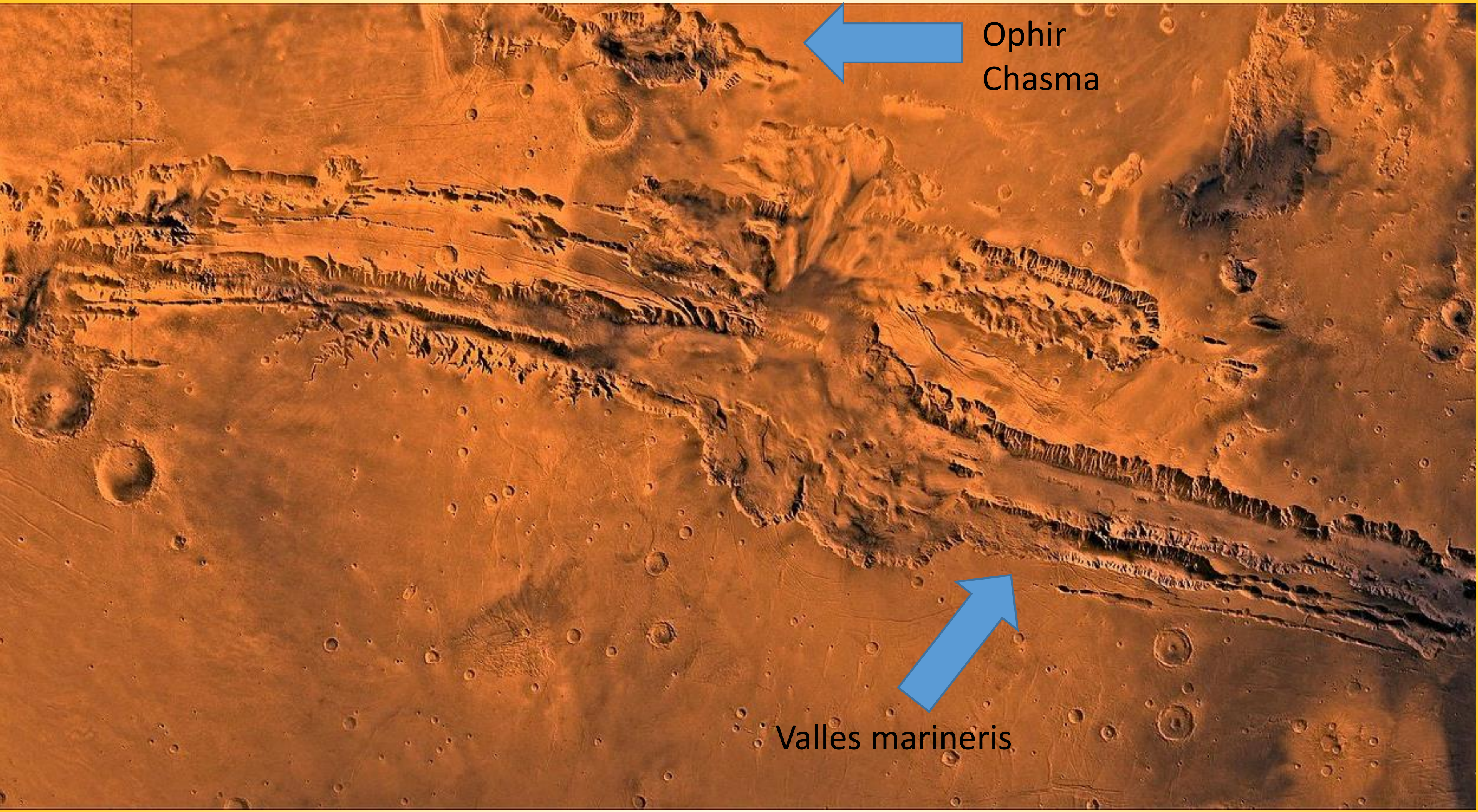

El área de la valles marineris es uno de los lugares donde esto procesos han sido mas activos

Brunetti, M.T., Guzzetti, F., Cardinali, M., Fiorucci, F., Santangelo, M., Mancinelli, P., Komatsu, G., **Borselli, L**., 2014. ***Analysis of a new geomorphological inventory of landslides in Valles Marineris, Mars***. Earth Planet. Sci. Lett. 405, 156–168. Doi:10.1016/j.epsl.2014.08.025.

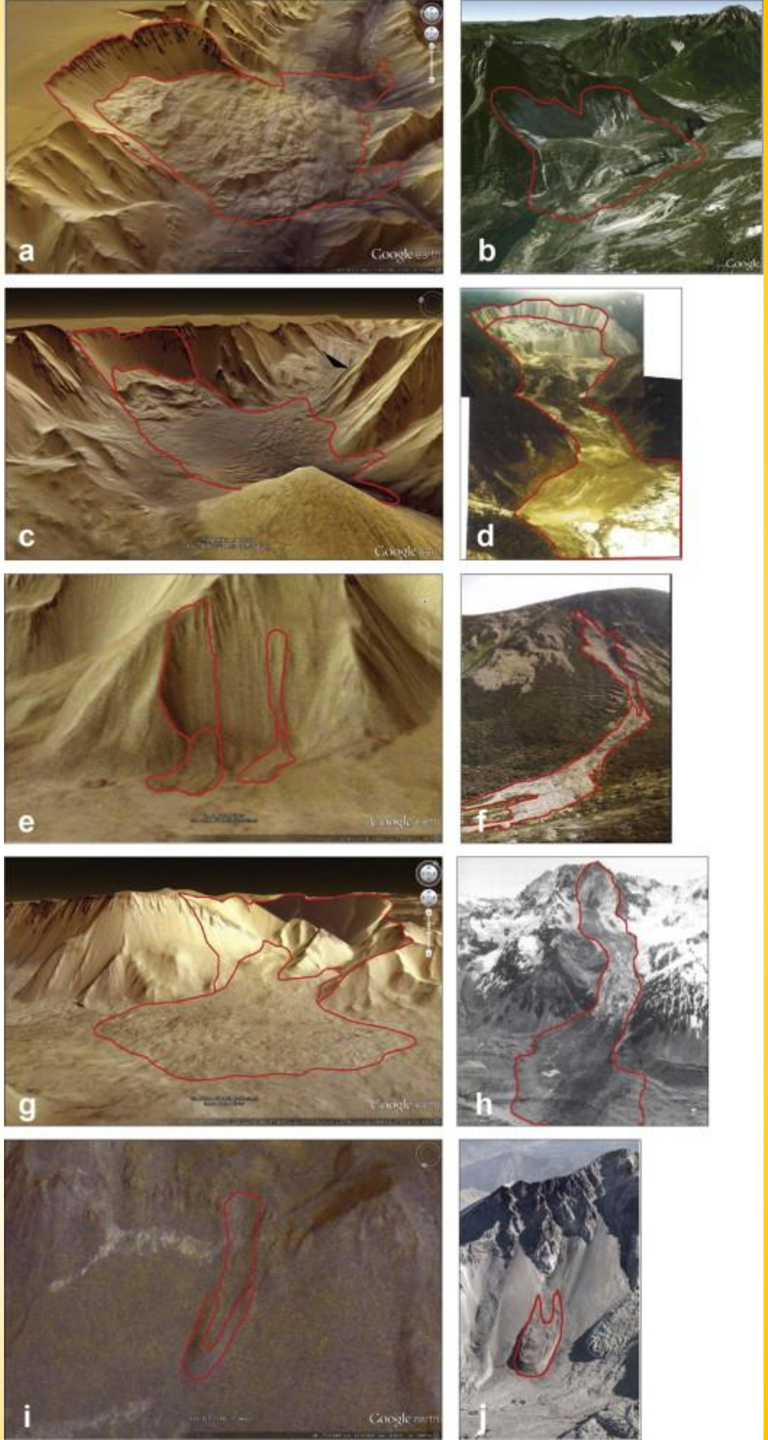

Comparison of mass wasting features detected and mapped in Valles Marineris, Mars (source: Google Mars™), with terrestrial analogous. (a) Rock slide (RS), and (b) Vajont rock slide, Mount Toc, Italy (source: Google Earth™); (c) complex/compound landslide (CL), and (d) Bairaman River landslide, Papua New Guinea (source: Landslides of the World, edited by K. Sassa, 1999); (e) debris flow (DF), and (f) Slochd Bheag debris flow, Ben Avon, Scotland (source: www.landforms.eu/cairngorms/debris_flow.htm); (g) rock avalanche (RA), and (h) Mount Cook rock avalanche, New Zealand (source: Landslides of the World, edited by K. Sassa, 1999); (i) rock glacier-like feature (RG), and (j) Mount Saint Helens rock glacier, Washington, USA (source: rockglacier.blogspot.com/2010/05/mount-st-helens-30-years-of.html).

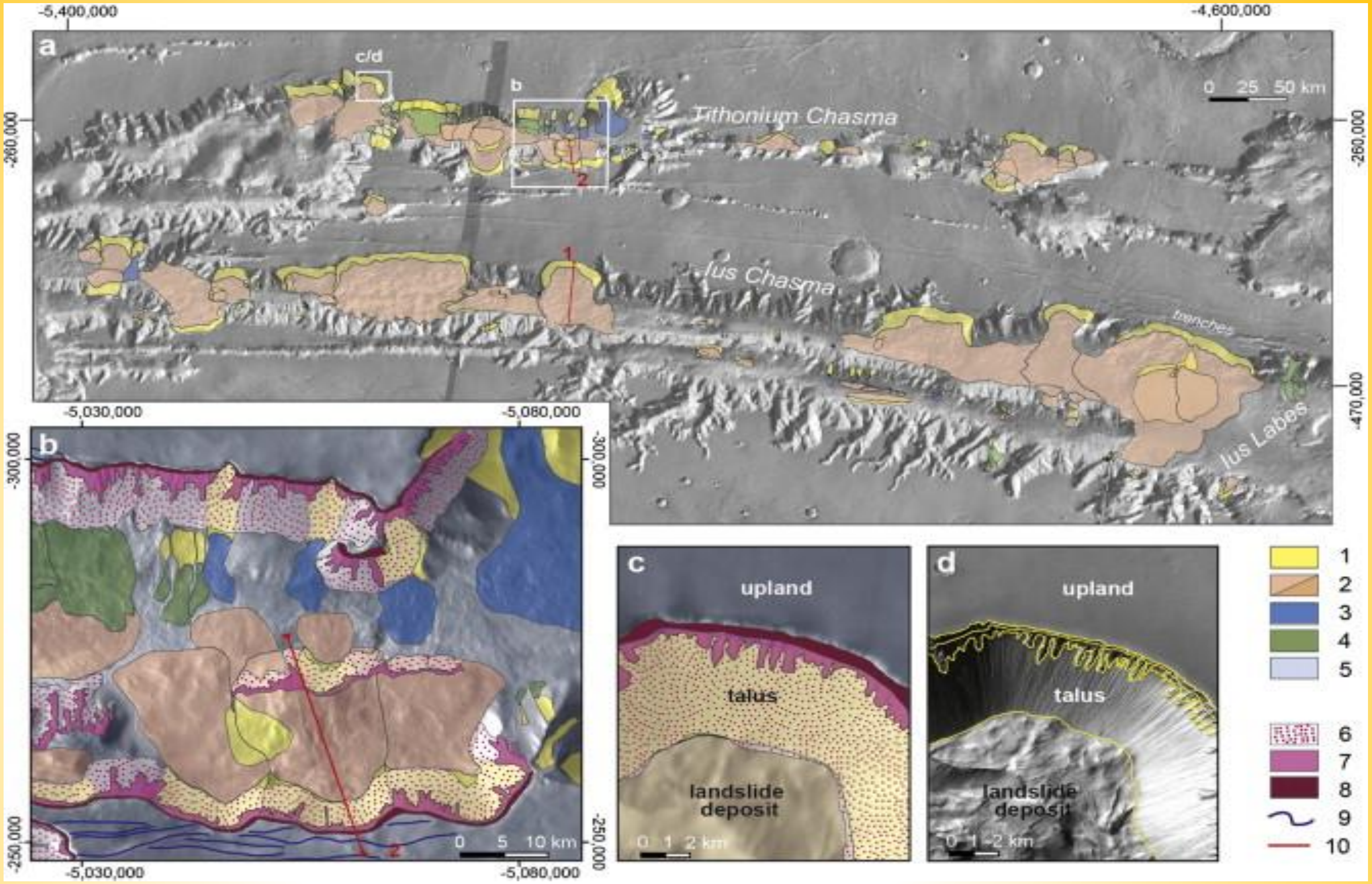

Brunetti et al. 2014.

Legend: (1) landslide scarp (source area). (2) Deposit of slide, including rock slides (RS), complex and compound failures (CL). Relative age shown by different shades of colour, from older (light) to younger (darker). (3) Deposit of rock avalanche (RA). (4) Debris flow (DF), including debris avalanches and shallow debris slides. (5) Rock glacier-like features (RG). (6) Talus. (7) Bedrock. (8) Rock cliff. (9) Surface trace of trench. (10) Position of profiles used in slope stability analysis

Brunetti et al. 2014.

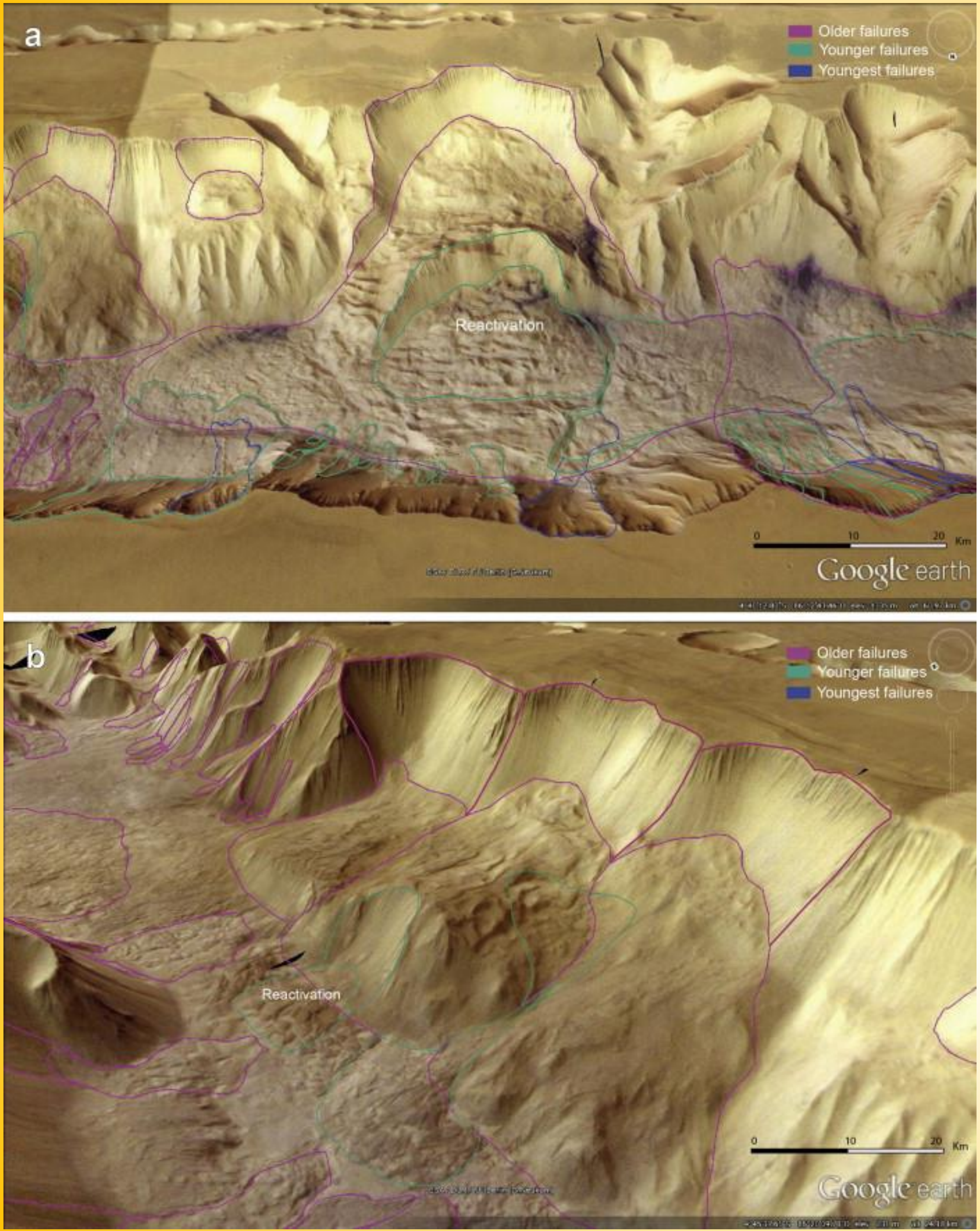

a) and (b) Maps showing multiple generations of slope failures in a portion of the study area. Purple contours are failures older than the green (younger) and the blue (youngest) landslides. Background shows HRSC mosaic (~15 m/pixel) draped on MOLA DEM (Christensen et al., 2004).

Mars – Ophir Chasma

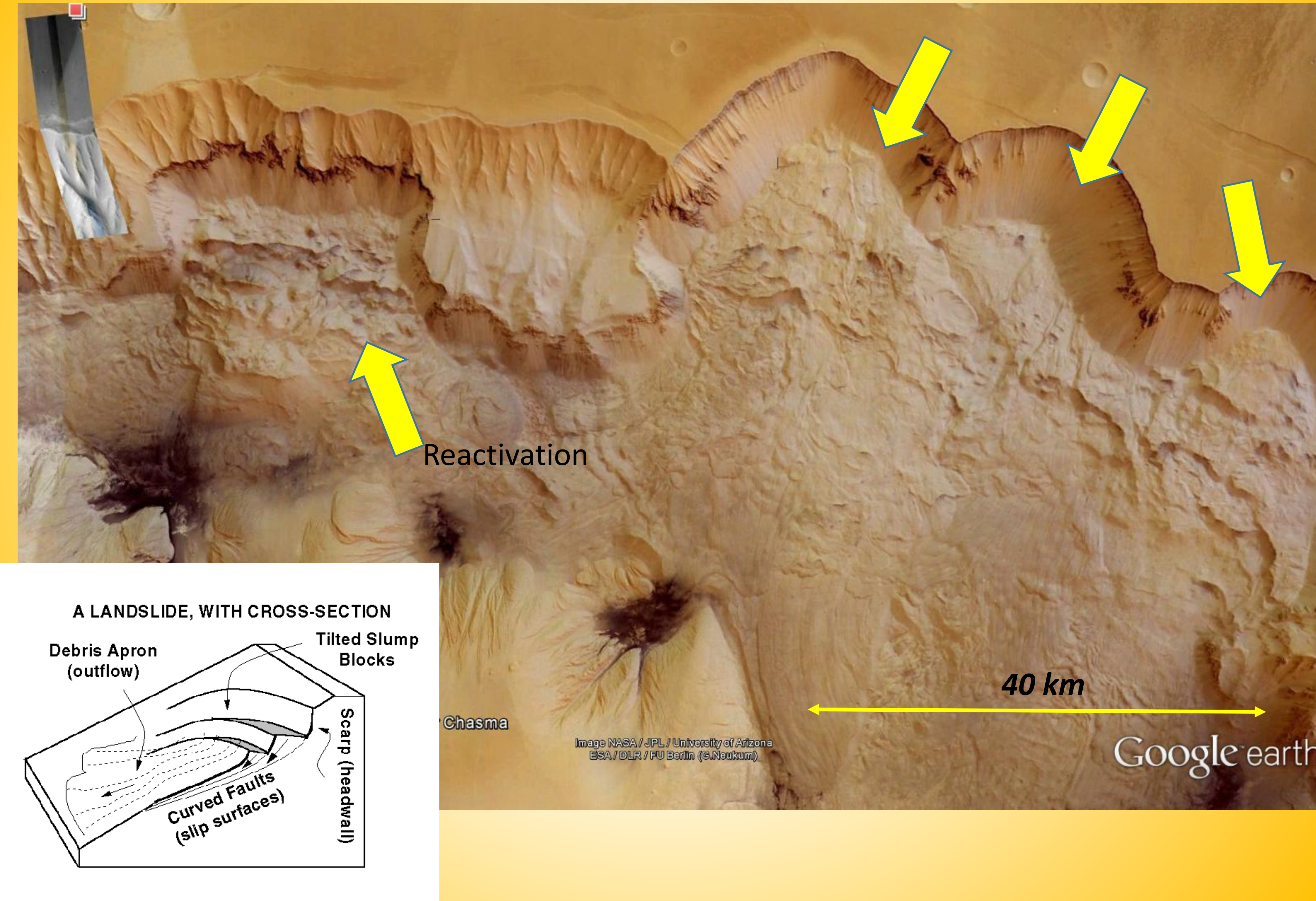

Mars – Ophir Chasma

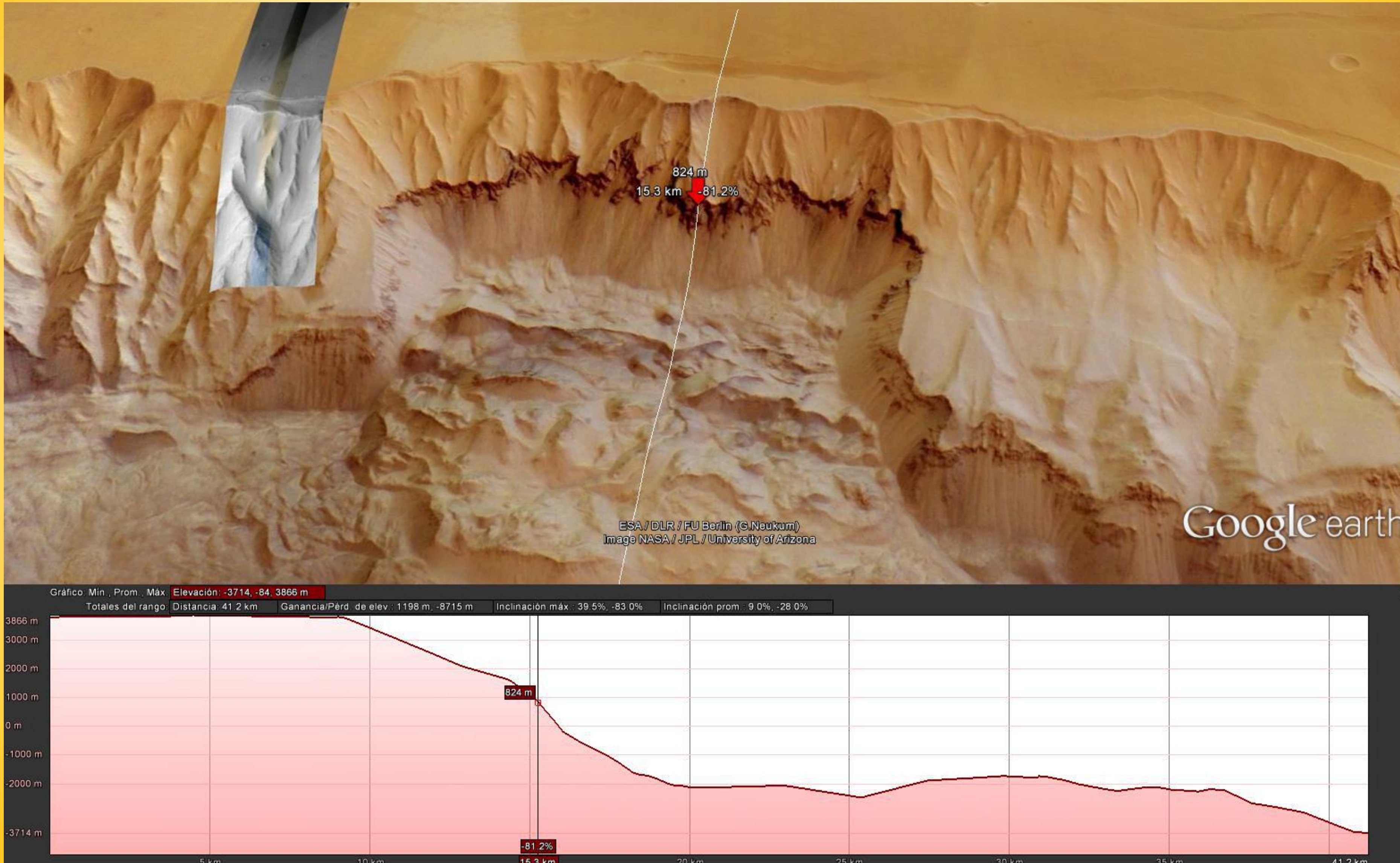

Mars – Ophir Chasma

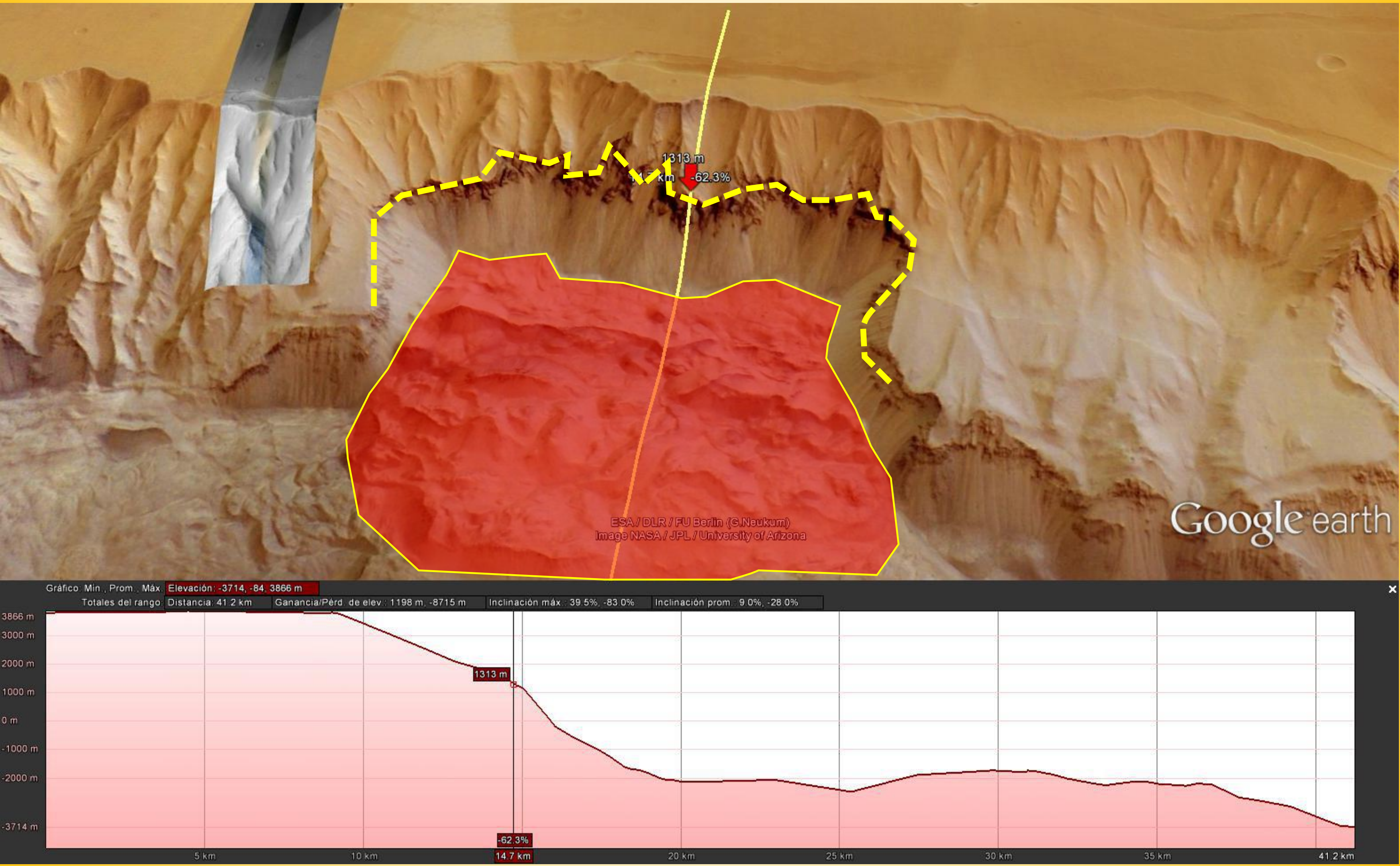

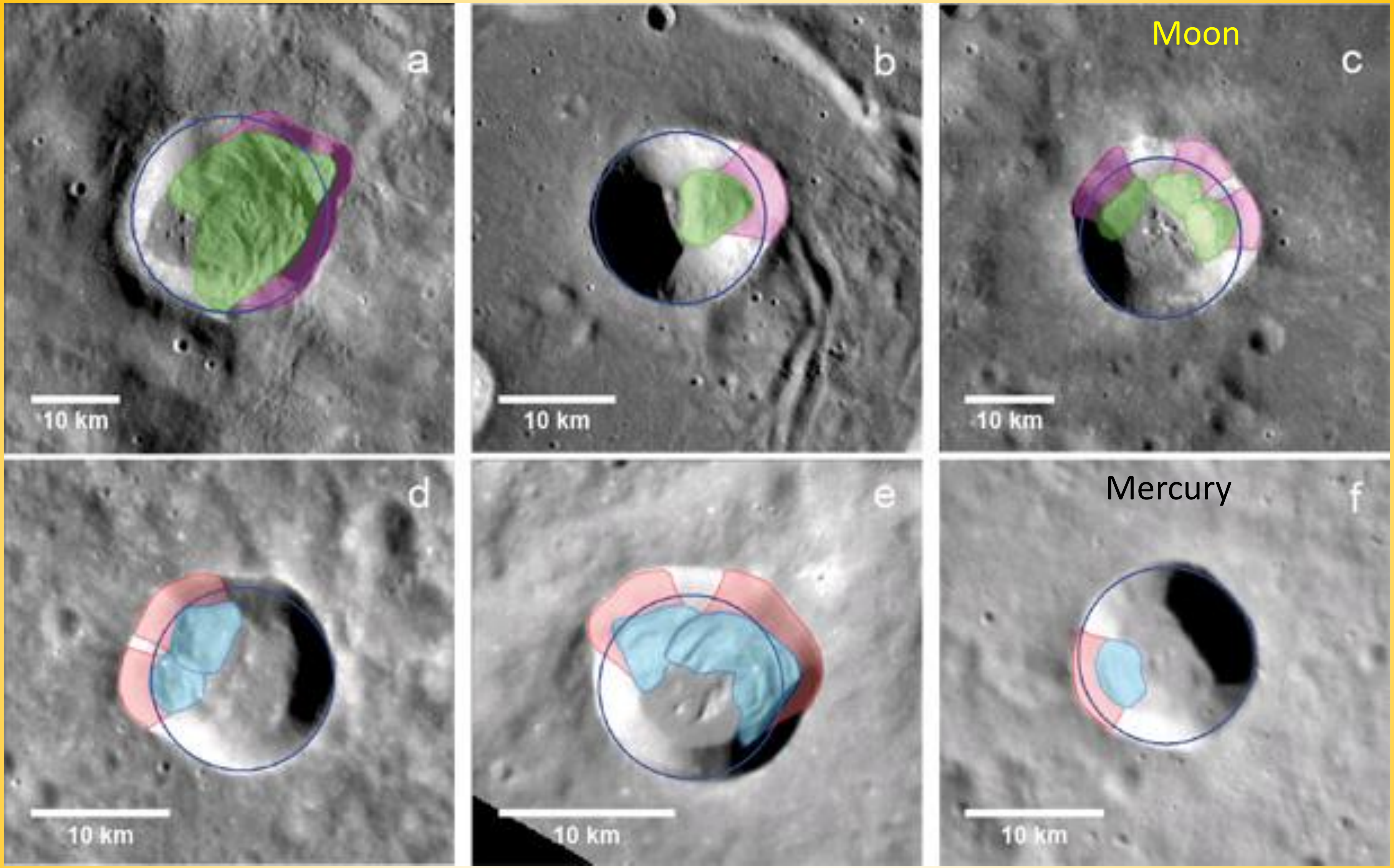

Examples of rock slides on the Moon (scarps in purple and deposits in green) and Mercury (scarps in red and deposits in light blue).

http://www.irpi.cnr.it/en/focus/frane-nel-sistema-solare-2/

Brunetti MT, Xiao Z, Komatsu G, Peruccacci S, Guzzetti F. 2015. Large rock slides in impact craters on the Moon and Mercury. *Icarus* 260: 289–300. [DOI: 10.1016/j.icarus.2015.07.014](https://doi.org/10.1016/j.icarus.2015.07.014).

Brunetti et al. 2014.

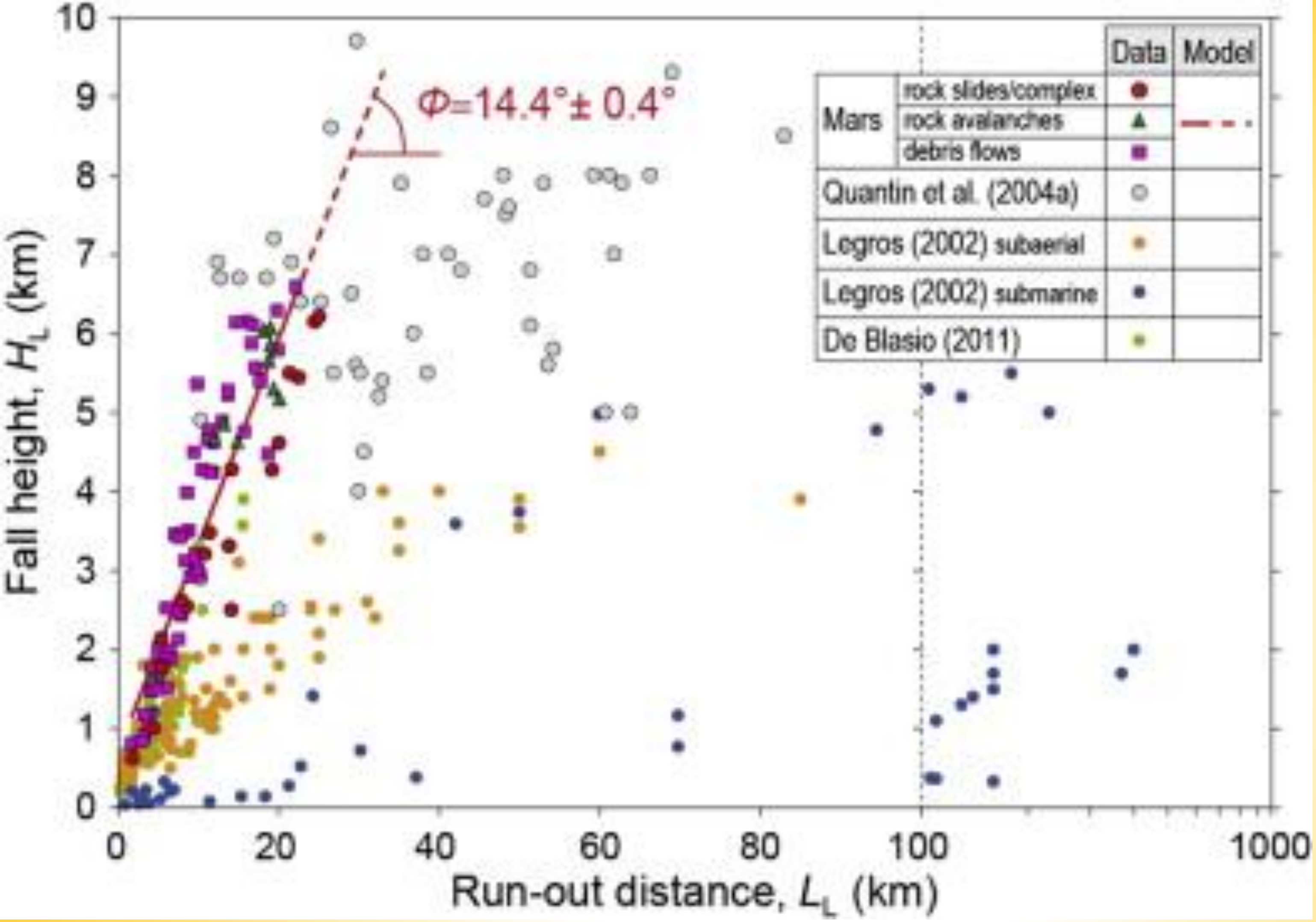

Dependence of landslide fall height H_L on run out distance L_L for 51 unconstrained landslides mapped in Tithonium and Ius Chasmata, Valles Marineris, Mars (this study), and for previously published Martian (Quantin et al., 2004a) and terrestrial (subaerial and submarine) failures (Legros, 2002 and De Blasio, 2011). Red line shows the relationship H_L=0.29×L_L obtained through linear fitting.

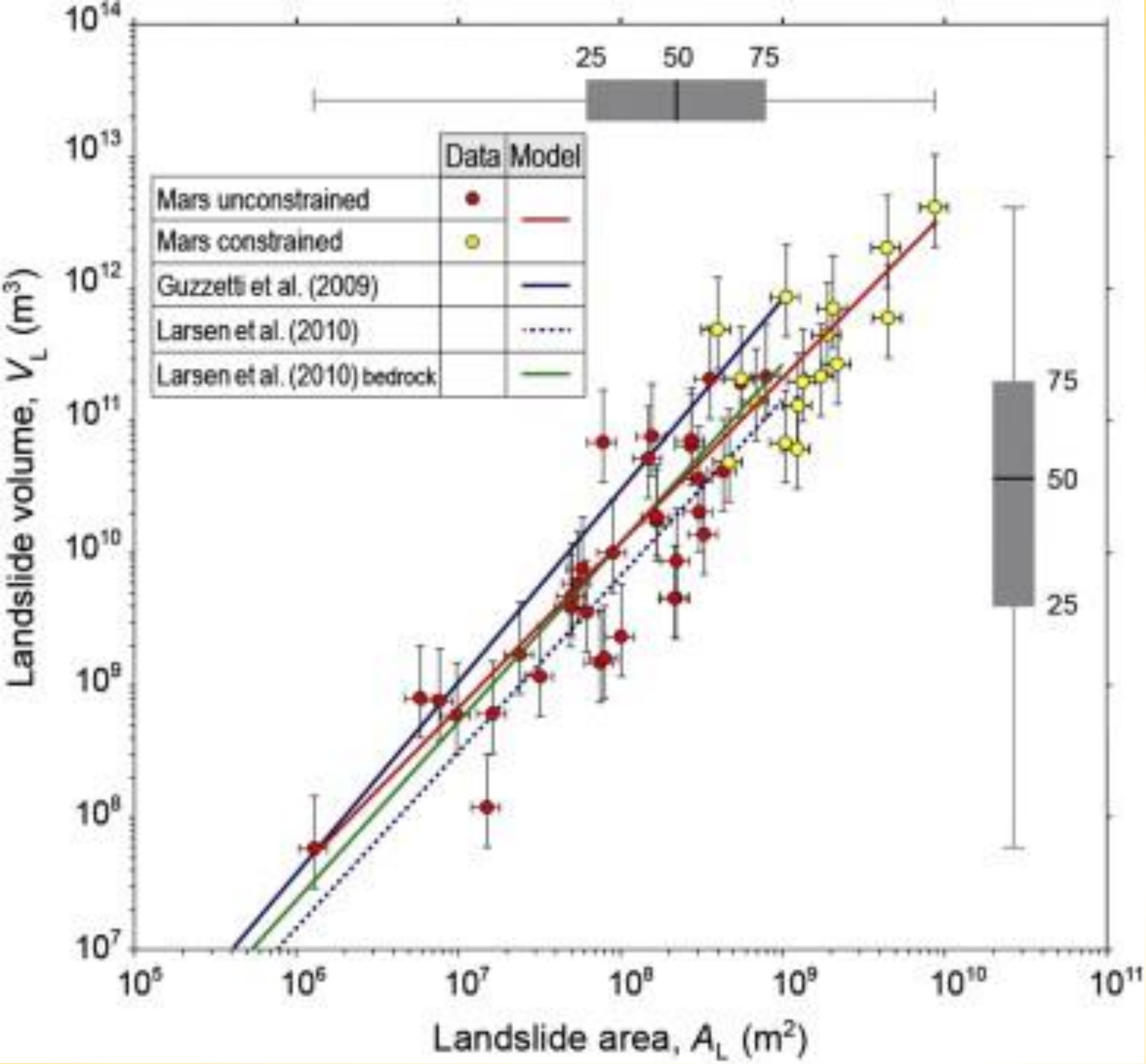

Dependence of landslide volume VL on landslide area AL for 49 landslides mapped in Tithonium and Ius Chasmata, Valles Marineris, Mars. Red dots show unconstrained landslides and yellow dots show landslides constrained by local topographic setting. Red line shows equation View the MathML source obtained though robust linear fitting. Solid and dashed blue lines, and green lines are similar relationships for terrestrial landslides (Guzzetti et al., 2009 and Larsen et al., 2010). Box plots show statistics of AL (right) and VL (top) for landslides in the VM.

Brunetti et al. 2014.

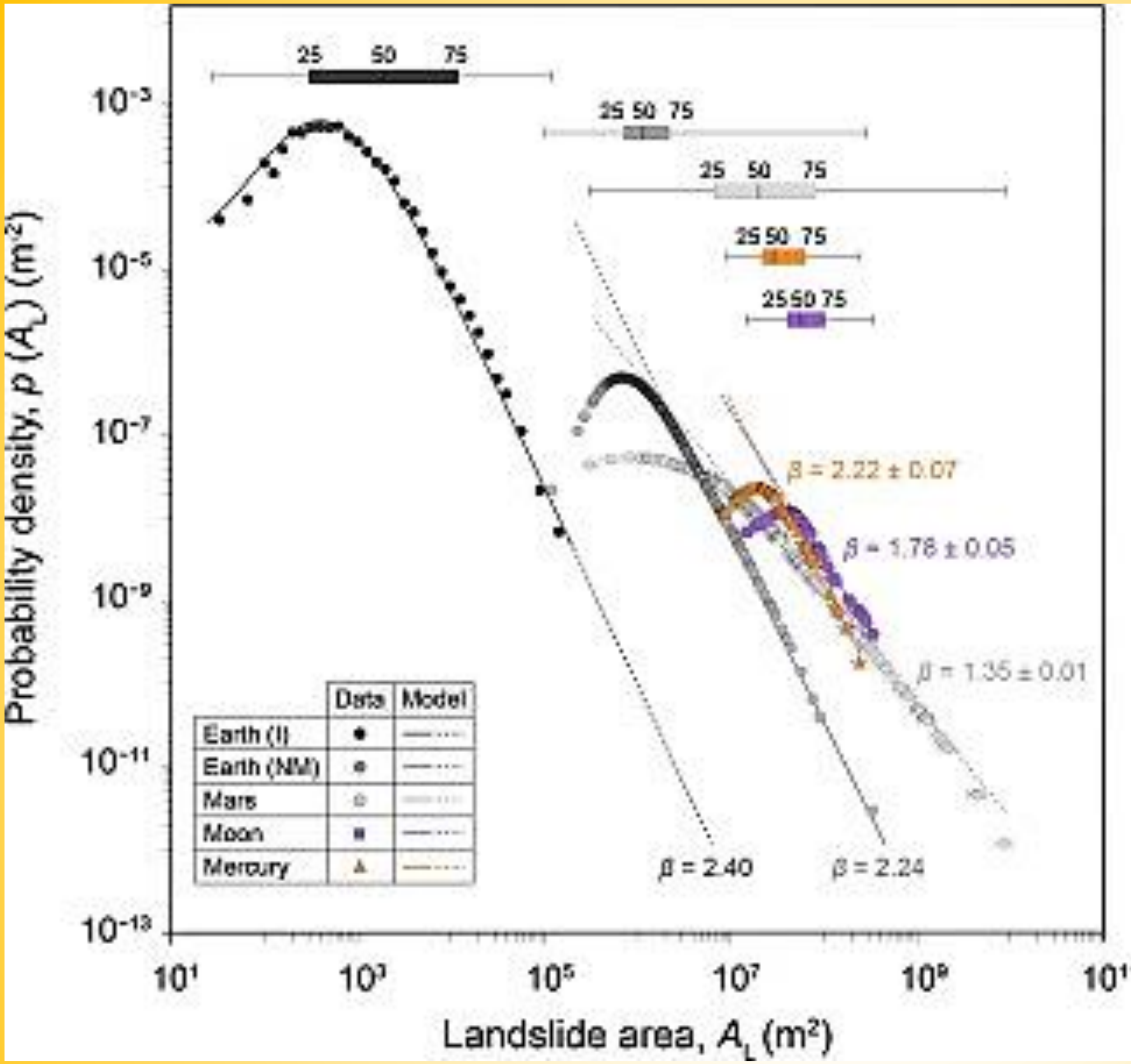

(Brunetti et al., 2015)

Probability distributions of landslide area on Earth, Mars, the Moon, and Mercury. p(AL) is the non-cumulative probability density of landslide area for 4233 terrestrial landslides (dark gray dots) triggered by a snowmelt event in Italy (Malamud et al., 2004), 894 terrestrial landslides (gray dots) in New Mexico (Cardinali et al., 1990), 198 landslides (light gray dots) on Mars (Brunetti et al., 2014), 60 rock slides on the Moon (purple squares), and 58 rock slides on Mercury (orange triangles) (this work). Color lines show corresponding best fit models of the distribution tails. Box plots show statistics of AL for all data sets

Results of slope stability analyses performed along two representative slopes in Tithonium Chasma (left charts) and Ius Chasma (right charts). (a) Dry slope and no external forcing. (b) Fully saturated slope (vertical blue bar) and no external forcing. (c) Dry slope and external seismic forcing (black arrow). (d) Fully saturated slope and external seismic forcing (vertical blue bar and black arrow). Each chart shows ten sliding surfaces with the smallest computed Factor of Safety (FS) obtained adopting a Limit Equilibrium Method approach. Blue lines show sliding surfaces with FS > 1 (stable conditions). Red lines show sliding surfaces with FS ≤ 1 (unstable conditions). Green lines show topographic profiles

Slope stability analysis

By SSAP software: www.ssap.eu

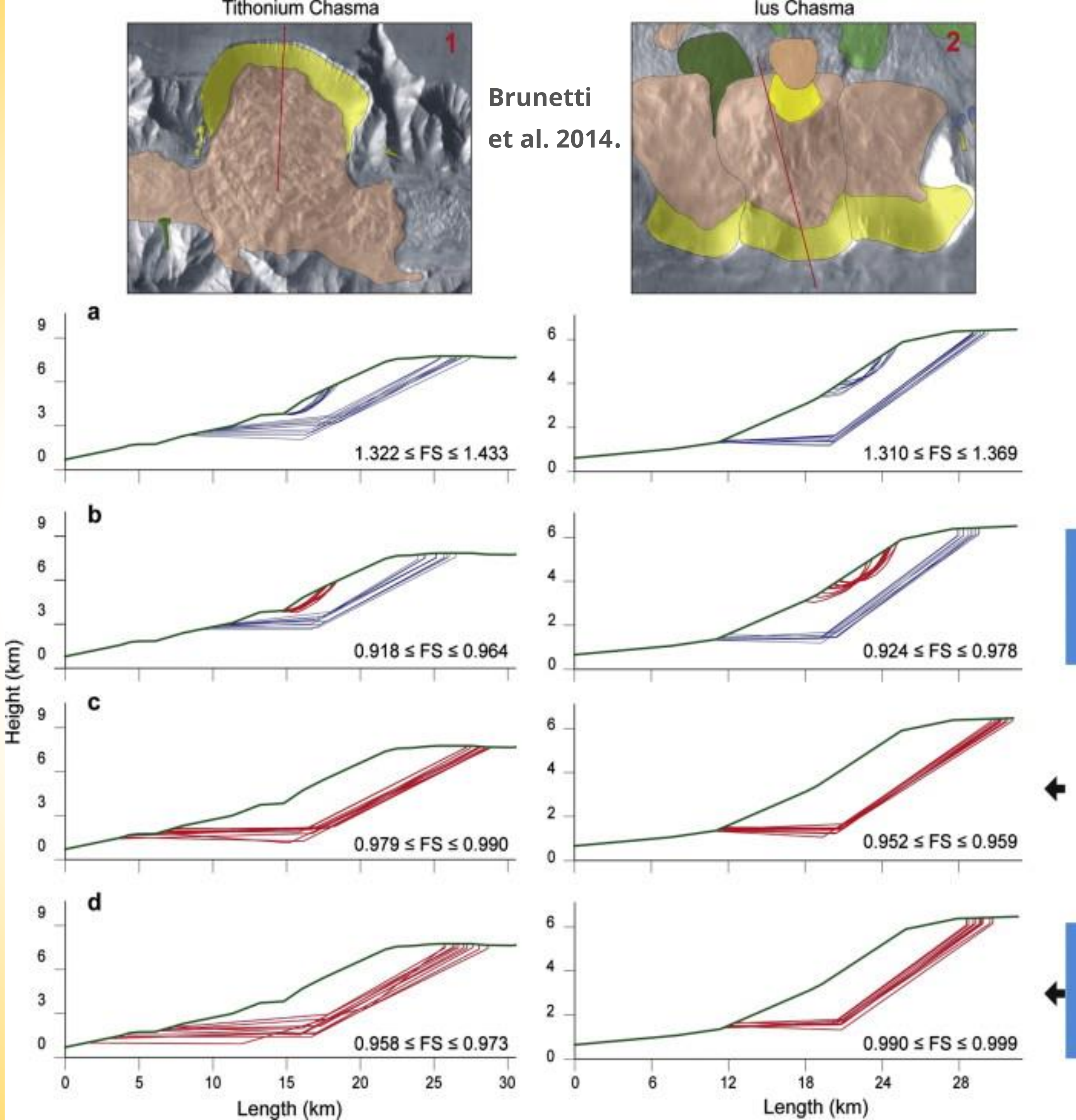

Geo-mechanical parameters used for the slope stability calculations in Tithonium and Ius Chasmata, Valles Marineris, Mars. Parameters related to rock mass strength criteria (Hoek et al., 2002). Used in SSAP software reléase 4.0.8

Parameter	Unit	Value
Surface gravity	$m\ s^{-2}$	3.7
Rock unit weight	$kN\ m^{-3}$	10.7
Water unit weight	$kN\ m^{-3}$	3.7
Water saturated rock unit weight	$kN\ m^{-3}$	11.1
Uniaxial compressive strength of intact rock[*]	MPa	90
Horizontal pseudo-static seismic coefficient, K_h	–	0.19–0.31
Geological Strength Index, GSI[*]	–	30–70
m_i value for basalt rock mass[*]	–	25
Disturbance factor, *D*[*]	–	1.0

En el Planeta enano CERES

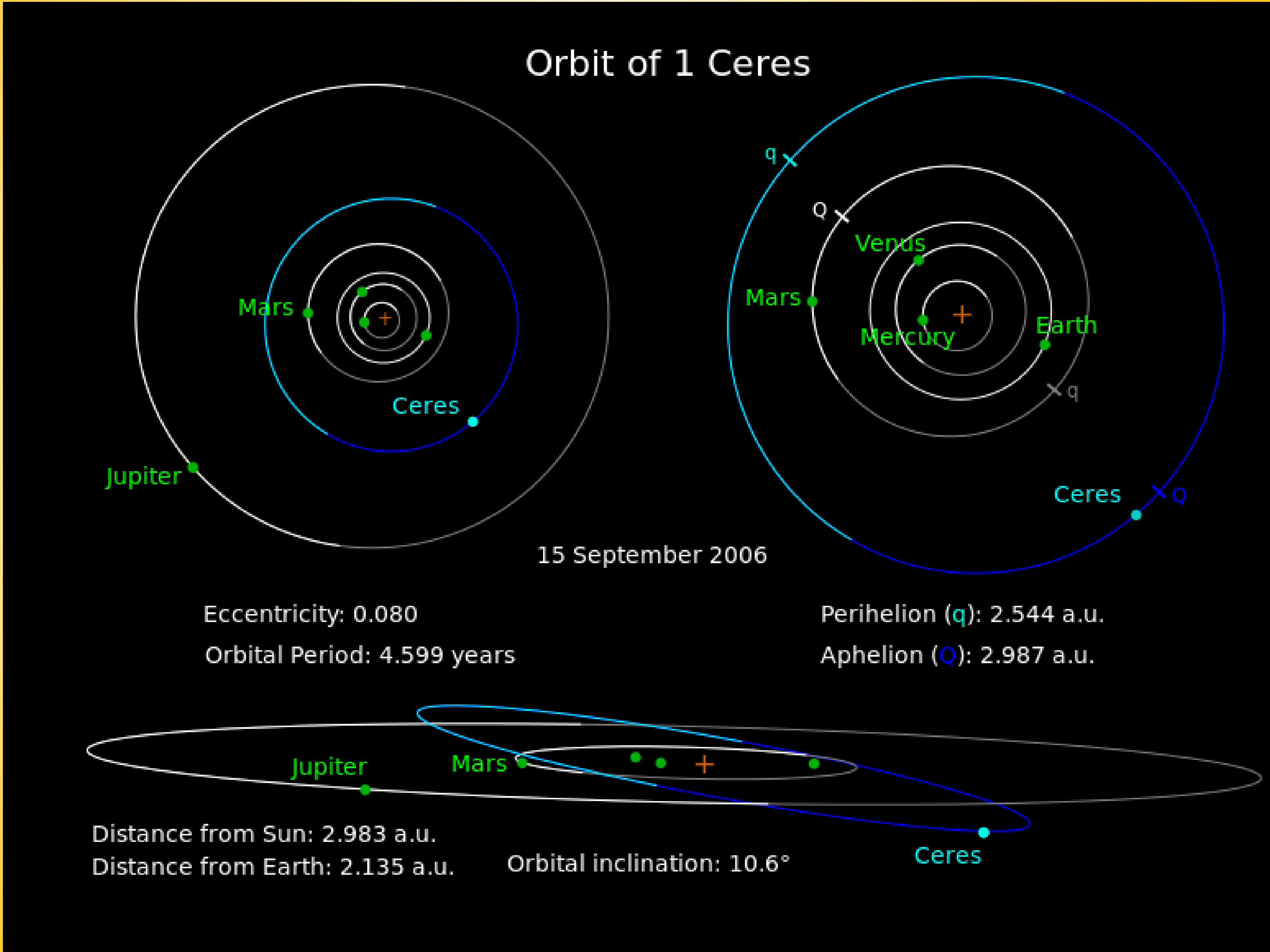

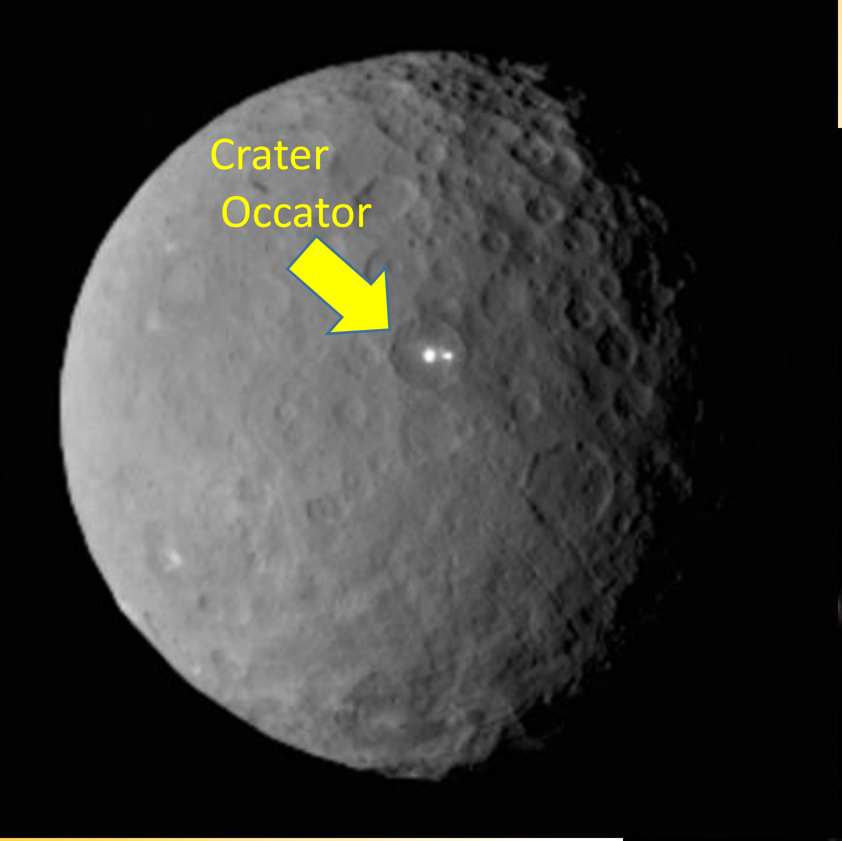

CERES imagenes sonda
Dawn 2015, JPL

Ceres Características físicas:

Dimensiones 974,6 x 909,4 km

Densidad 2,077±0,036 g/cm³

Área de superficie 2 850 000 km²

Diámetro promedio 952,4 km

Gravedad 0,28 m/s2 = 0,029 g ← Approx. 1/30 de la gravedad terrestre.

Características atmosféricas

Temperatura

Media ≈ 168 K

Máxima 235 K (-38° C)

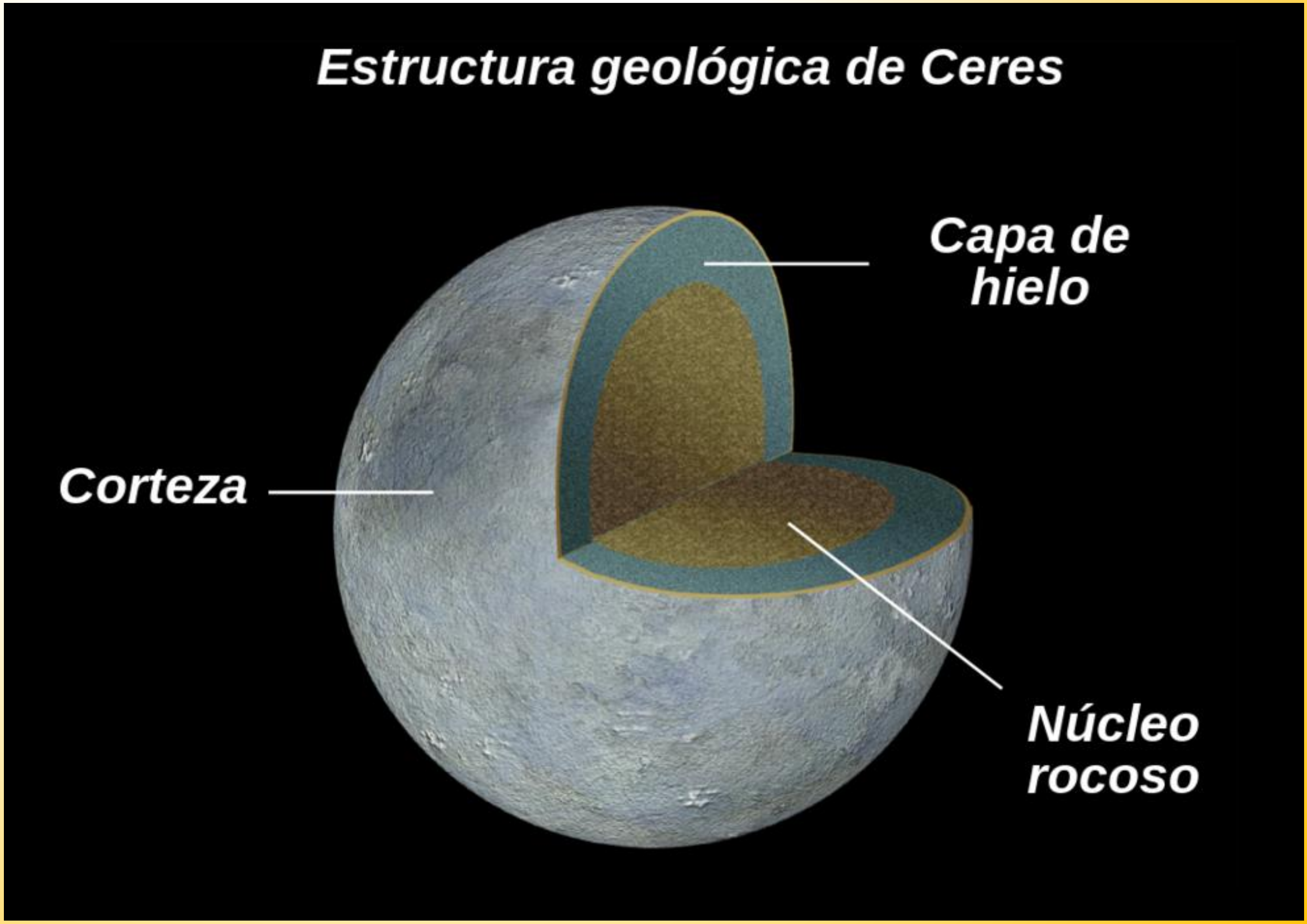

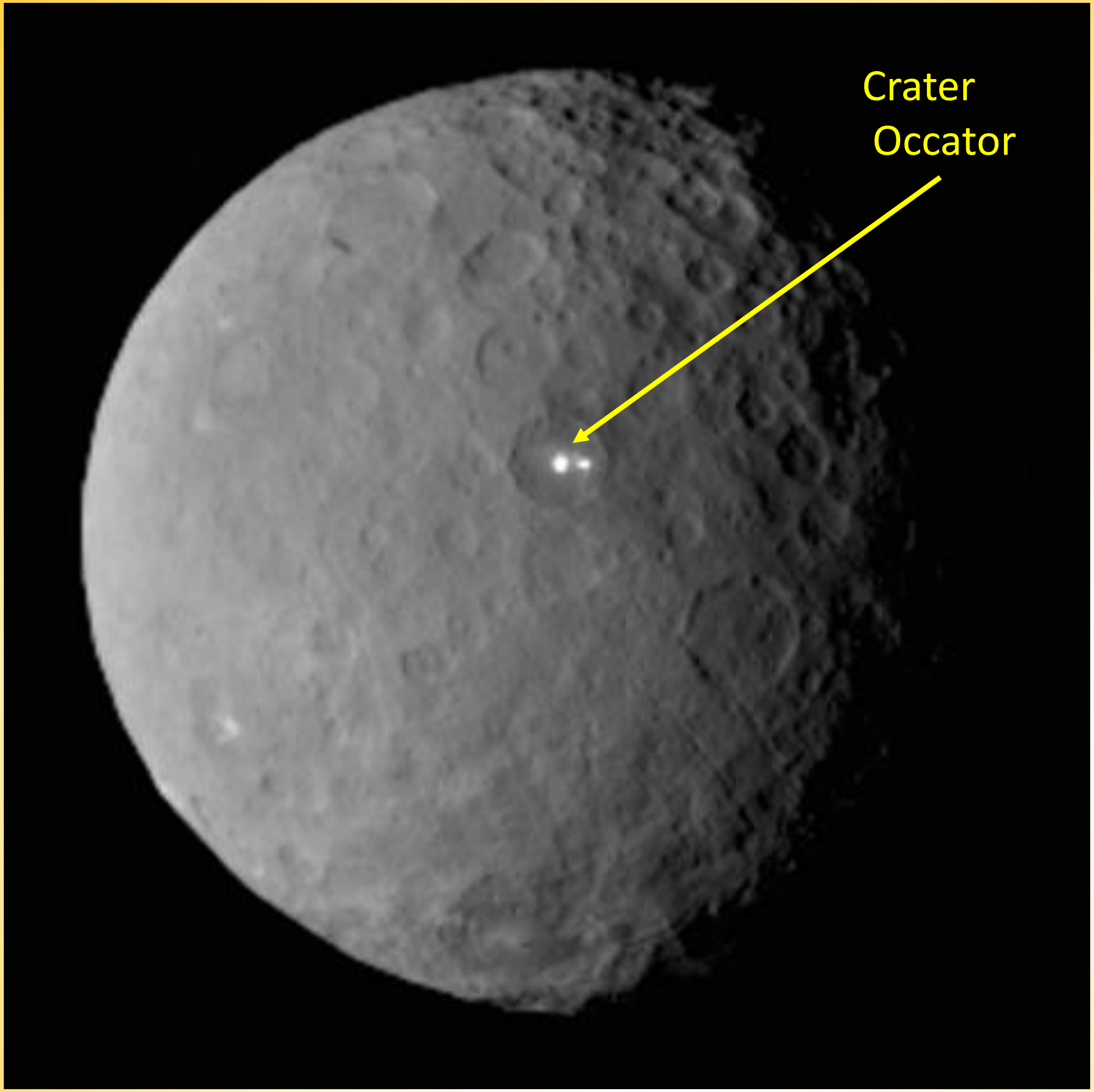

https://upload.wikimedia.org/wikipedia/commons/b/b3/Ceres_RC2_Bright_Spot.jpg

Aunque los planetologos son mas interesados a los probable domos de hielo en el centro del cráter..

Pero Es igualmente interesante lo que pasa en la parte oeste del mismo crater

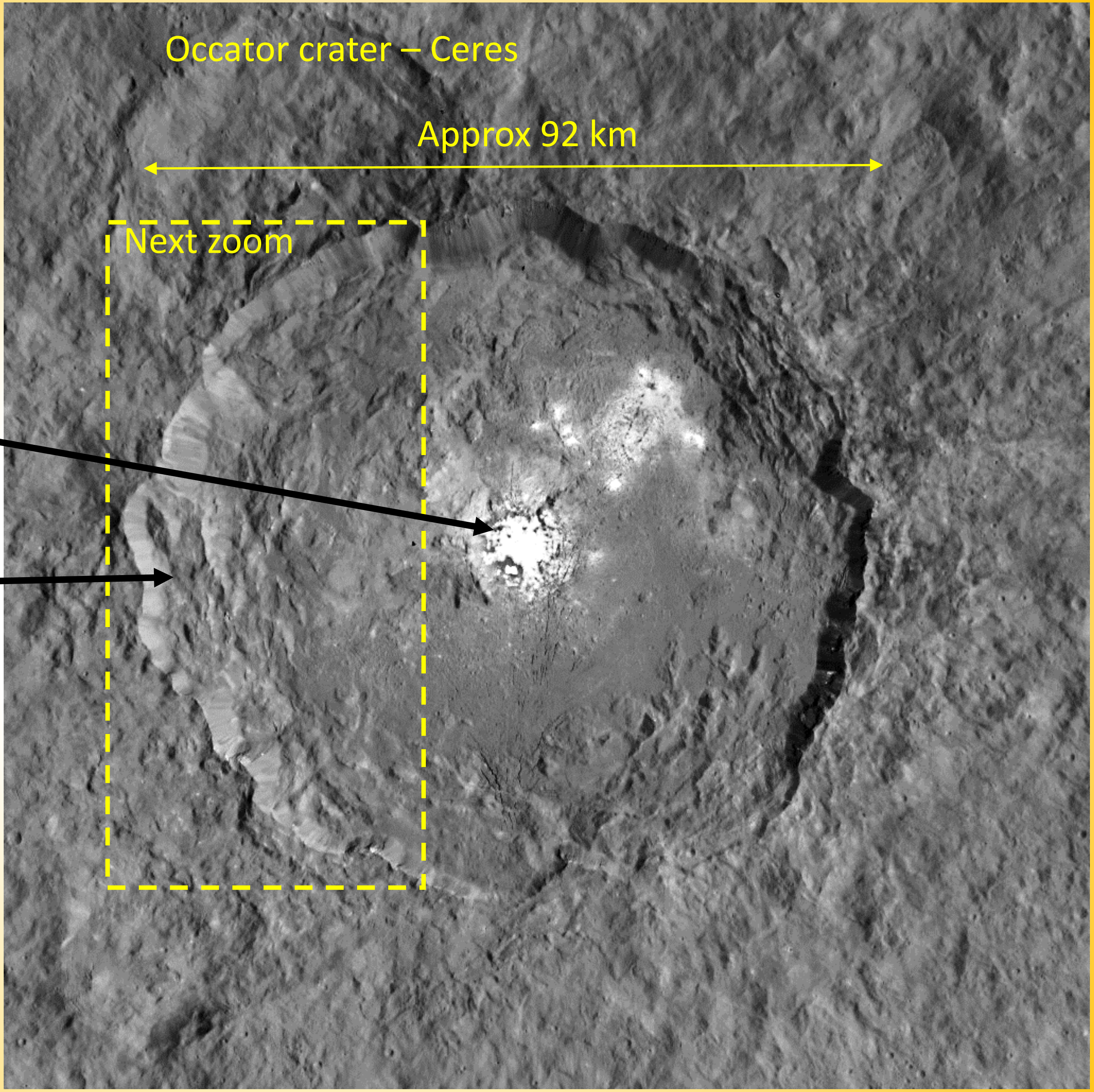

Image by http://www.jpl.nasa.gov/spaceimages/details.php?id=PIA19889

Occator cráter- detalle – Ceres

Images by http://www.jpl.nasa.gov/spaceimages/details.php?id=PIA19889

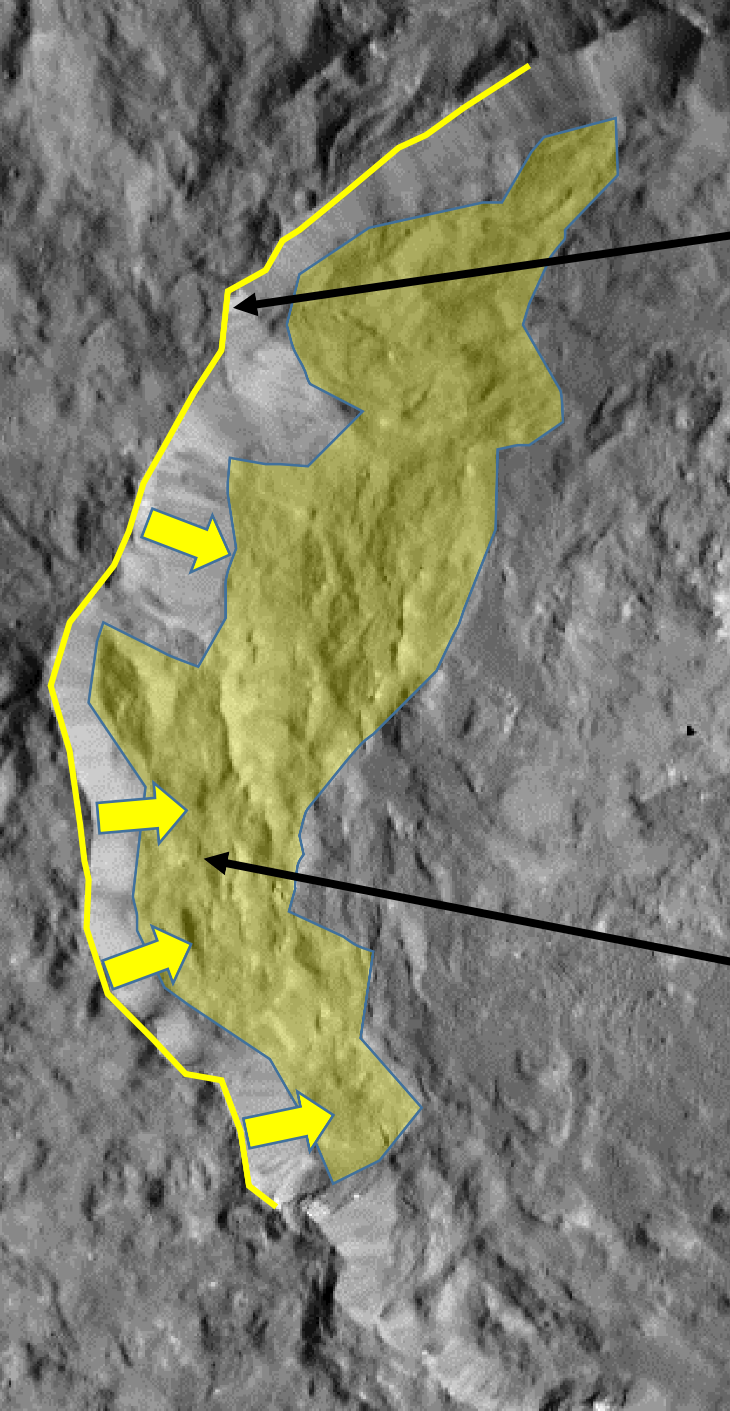

Corona
de deslizamiento

Accumulacion de
los deslizamiento
Con *hummoks*

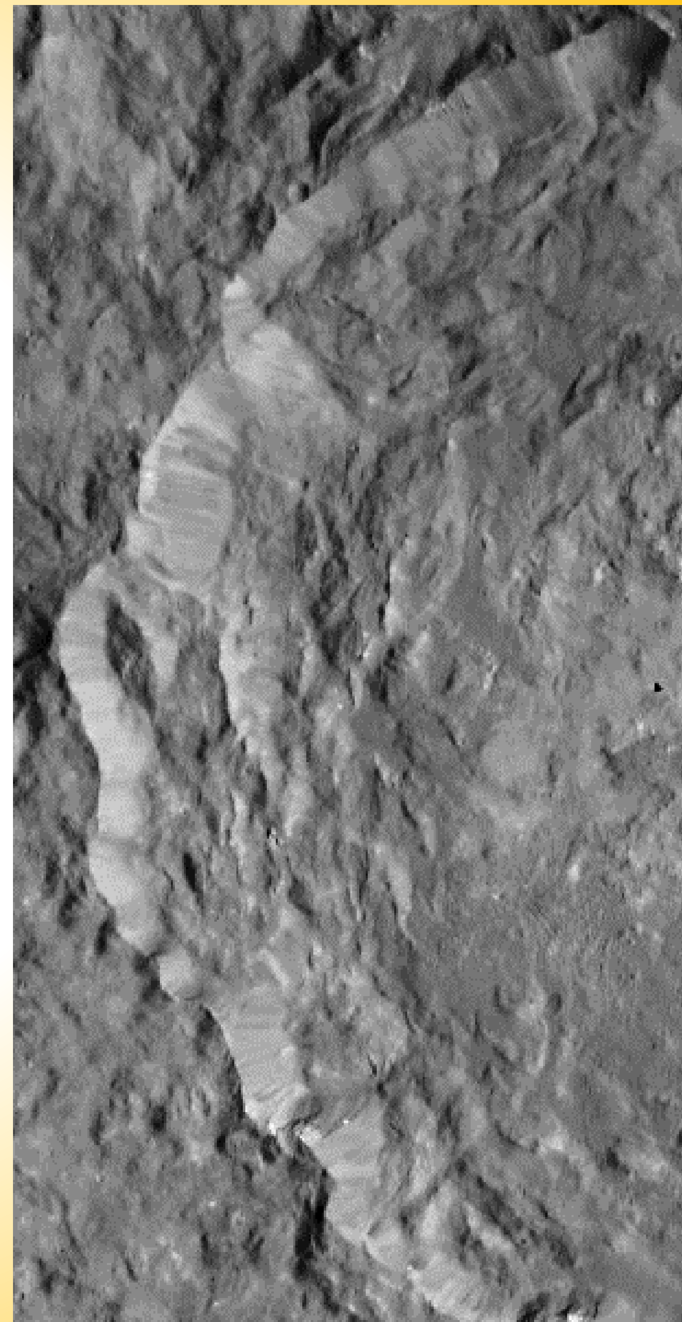

Volcanes terrestres
Y sus inestabilidades


Colima Volcano - 2011

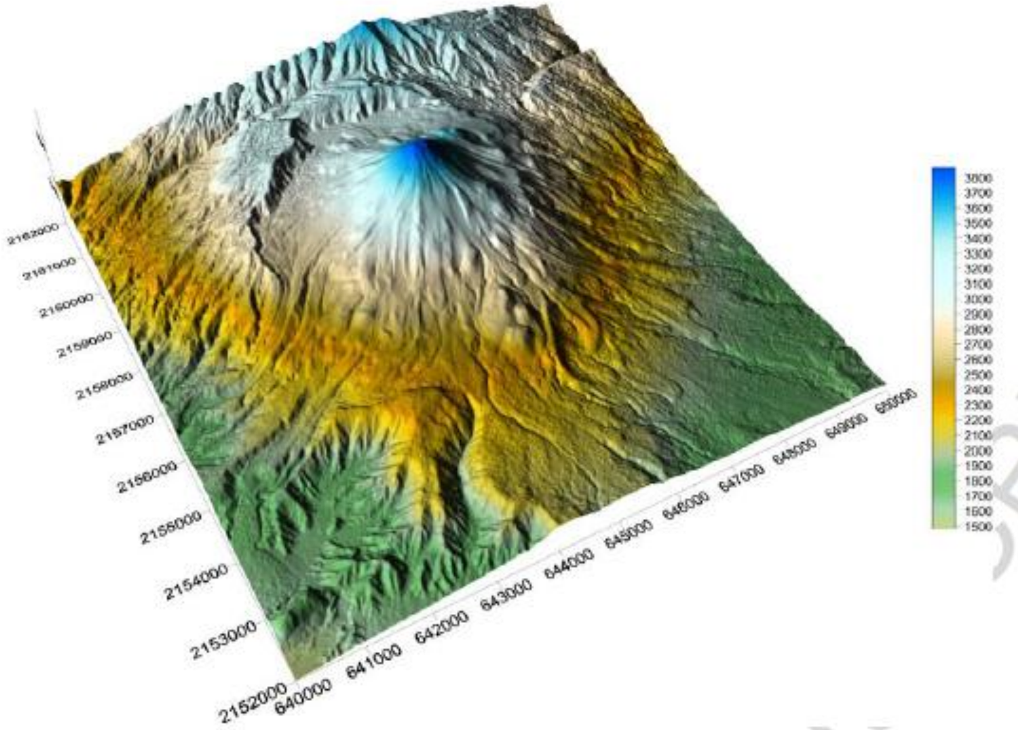

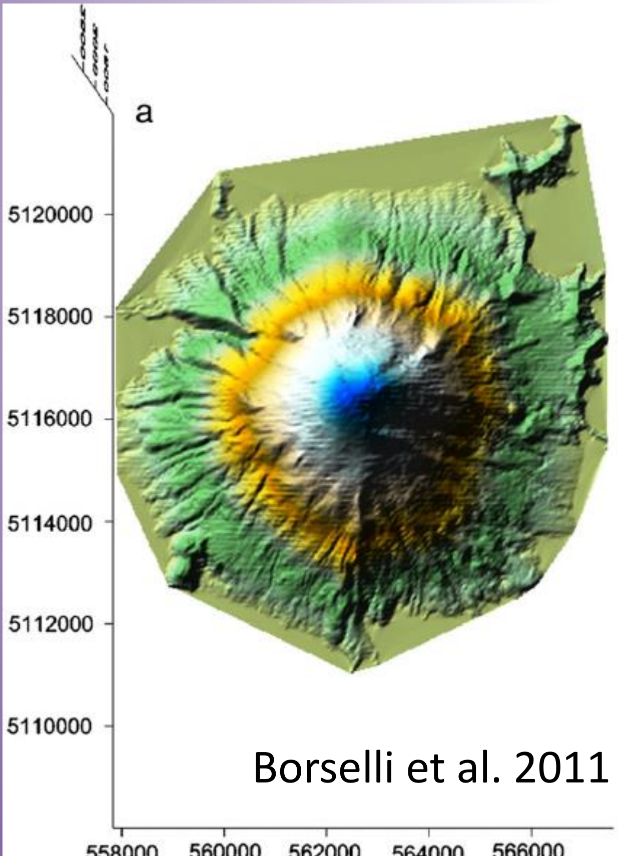
a
5120000
5118000
5116000
5114000
5112000
5110000
558000
560000
562000
564000
566000
Borselli et al. 2011


Mt. St. Helens - 1979

Collapso de sectore de volcanes

En 1980 el **colapso sector and avalancha del Mount St. Helens disparó el estudio de muchos deposito de avalancha similares en todo el mundo** (Siebert, 1984; Ui and Glicken, 1986; Siebert et al., 1987; Francis and Wells, 1988; Vallance et al., 1995).
Un resultado ahora consolidado de la volcanología del fin del siglo XX es que muchos volcanes son susceptibles de tener un colapso de estructura disparado da varios factores endógenos y exógenos exógenos (McGuire, 1996),

Mt. St. Helens - 1980

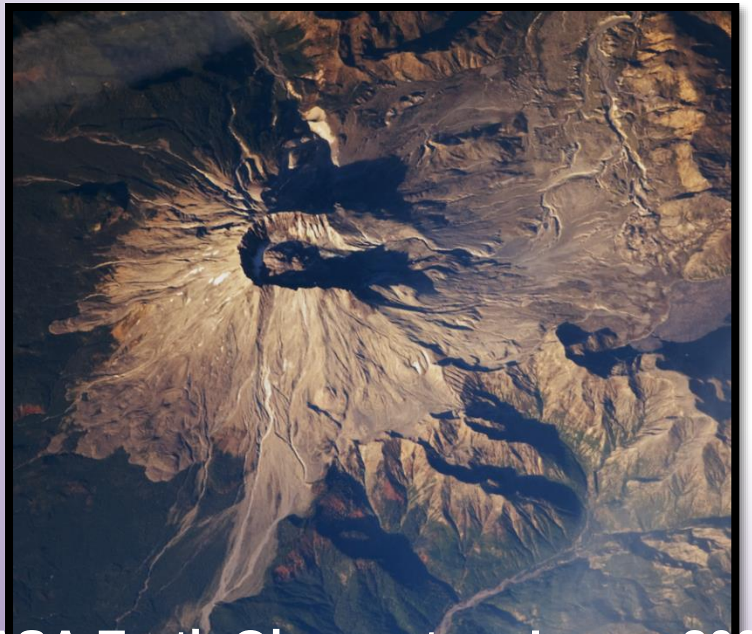

NASA Earth Observatory Image 2009

Colapso de sector de volcanes: causa de disparo

La inestabilidad de un edificio volcánico puede ser causada por muchos factores:

- intrusión magmática directa en el edificio (actividad de tipo Bezymianny, Gorshkov de 1962 Día, 1996; Elsworth y Voight, 1996),
- deposición de depósitos piroclásticos voluminosos en pendientes muy elevadas (Maguire, 1996),
- procesos hydromagmáticos (Dzurisin, 1998),
- actividad phreatomagmatic (actividad de tipo Bandai, Moriya, 1980).
- Actividad tectónica y fallas (McGuire, 1996; Siebert, 1984)
- Terremoto (Keefer, 1984)
- collapso gravitacionales pueden ocurrir en respuesta a un debilitamiento progresivo de un edificio.

Otros mecanismos de activación incluyen explosiones freáticas , precipitaciones extremas por huracanes (colapso en el volcán Casita en Nicaragua en 1998, Sheridan et al., 1999;. Scott et al, 2005).

Una nueva tecnica de studio que se aplica a stratolcanes A **recently developed technique** of analysis applied to stratovolcanoes by Borselli et al. (2011)*, para evaluar el grqado de inestabilidades de edificios volcanicos.

**BORSELLI L., CAPRA L., SAROCCHI D., De La CRUZ-REYNA S. (2011). Flank collapse scenarios at Volcán de Colima, Mexico: a relative instability analysis. Journal of Volcanology and Geothermal Research. 208:51–65.*

La nueva técnica combina tres metodologías :

- 1) **slope stability by advanced limit equilibrium analysis (ALEM) of multiple sectors on the volcano** using **SSAP 4.0** (***Slope Stability Analysis Software***, Borselli 2011) which include fluid internal overpressure or progressive dissipation (Borselli et al. 2011), and rock mass strength criteria (Hoek et al. 2002,2006) for local, stress state dependent, shear strength;

- 2) the analysis of **relative mass/volume deficit in the volcano structure**, made using the new **VOLCANOFIT 2.0** software (Borselli et al.2011);

- 3) **Statistical analysis of major flank debris avalanche ages in the last 20,000 BP**, using **stochastic arithmetic methods** (Vignes, 1993), and calculating the mean time of recurrence of them.

Relative slope stability by <u>advanced limit equilibrium method</u> (ALEM)

Limit equilibrium method (LEM) Slope stability analysis (Duncan 1996): Calculation of **Factor of Stability (FS)** which is associated to each section of volcanic edifice

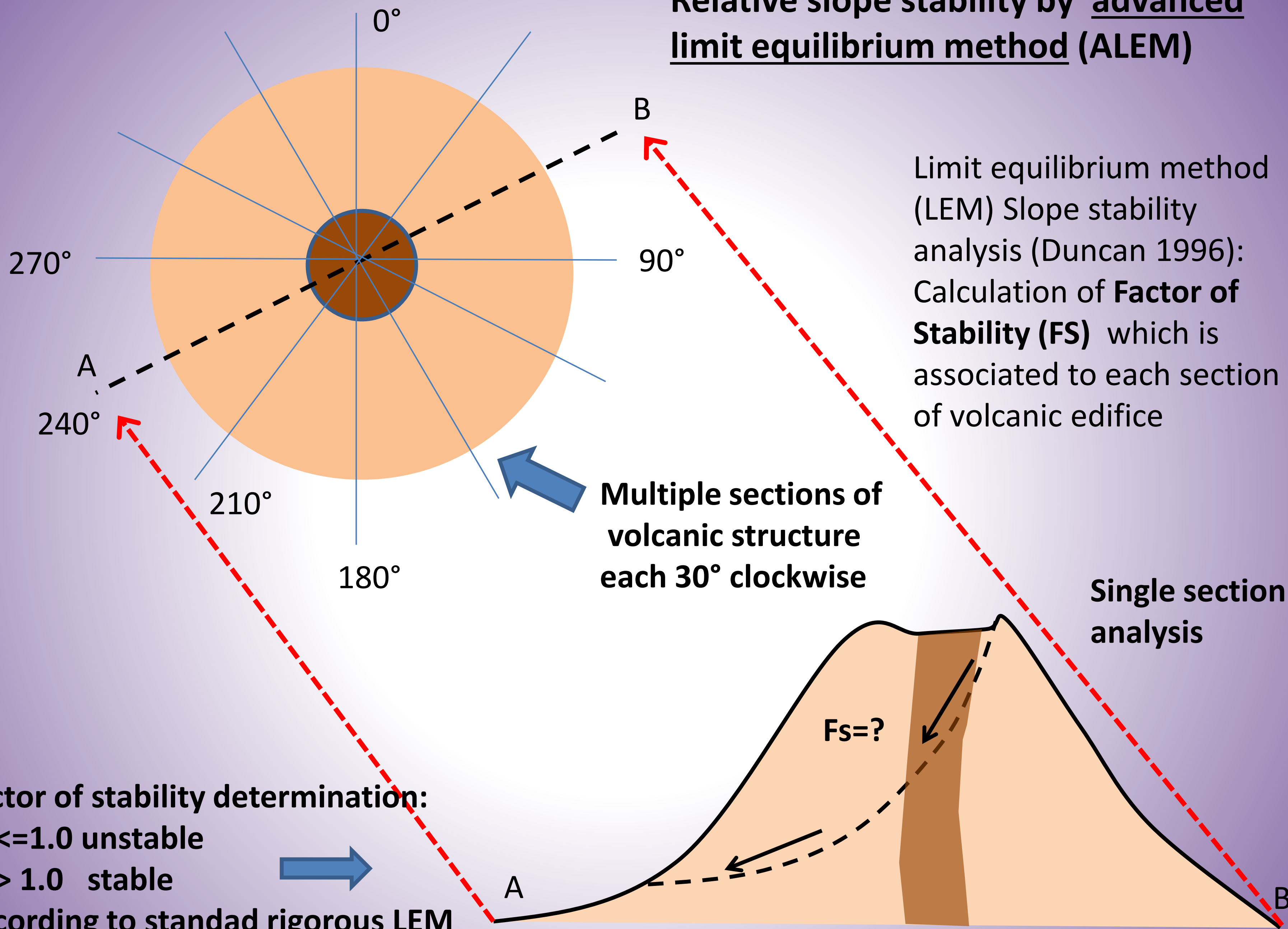

Factor of stability determination:
Fs <=1.0 unstable
Fs > 1.0 stable
According to standad rigorous LEM

Advanced LEM in SSAP 4.x

SSAP 4.7.2 is a full freeware software
http://www.ssap.eu
(Borselli 1991, 2016)

- Generic shape random search of minimum FS sliding surface by Monte Carlo method of generic shape (not only circular shape)
- Only Rigorouus LEM method
- Rock mass strength criterion (Hoek et al. 2002,2006).
- Fluid pressure function (overpressure and dissipation fields Inside volcanic edifice) (Borselli et al. 2011)

$$\sigma_f = \gamma_w z F_D + U_{0_{MIN}}$$

$$F_D = 1 - Ae^{-kD}$$

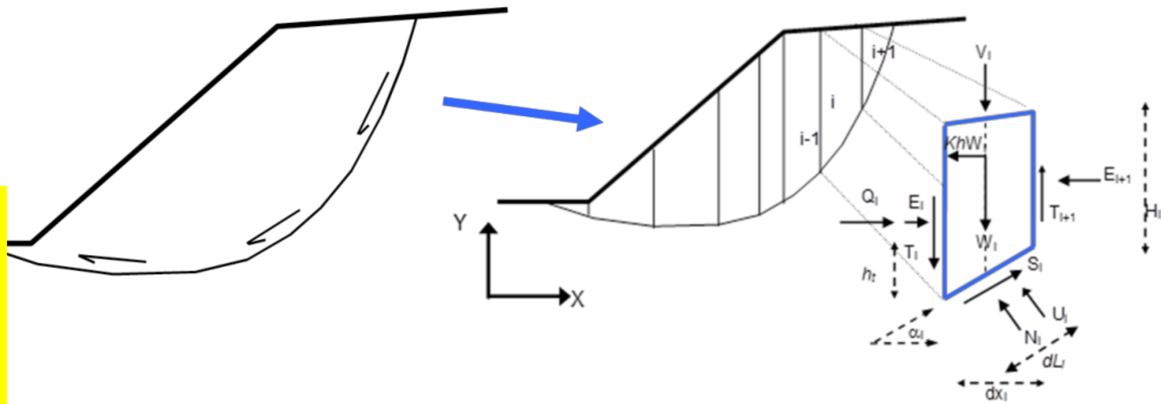

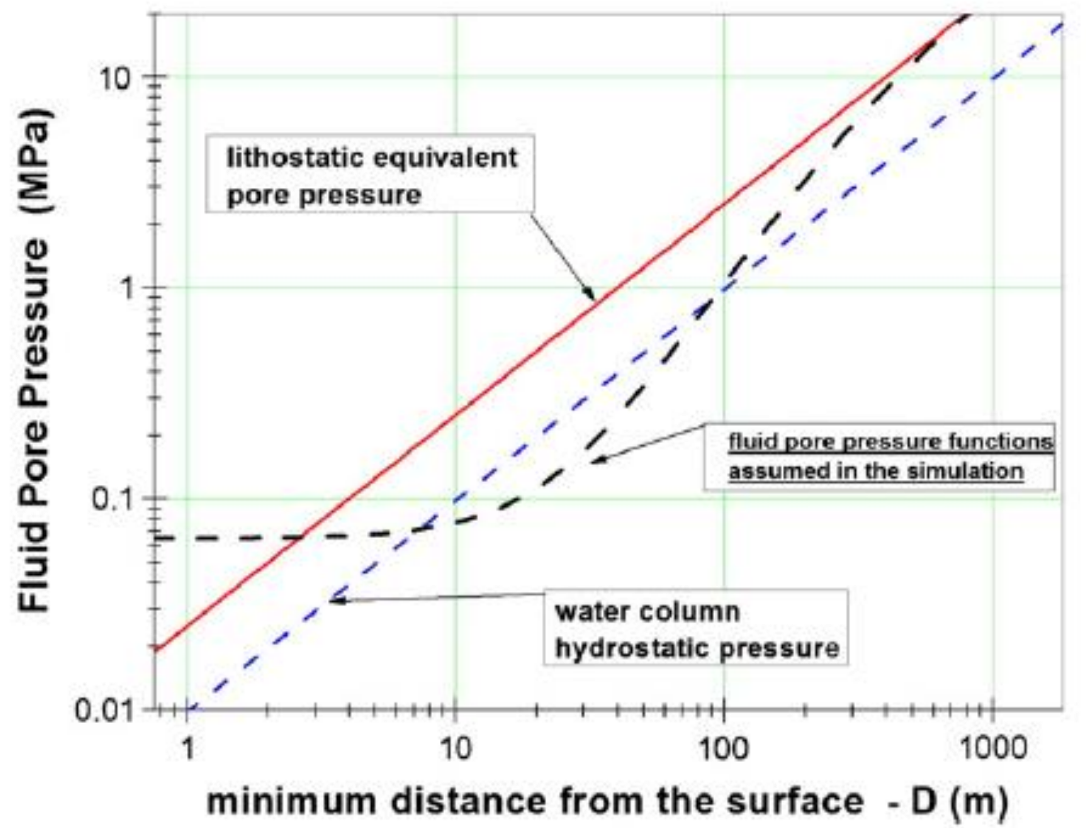

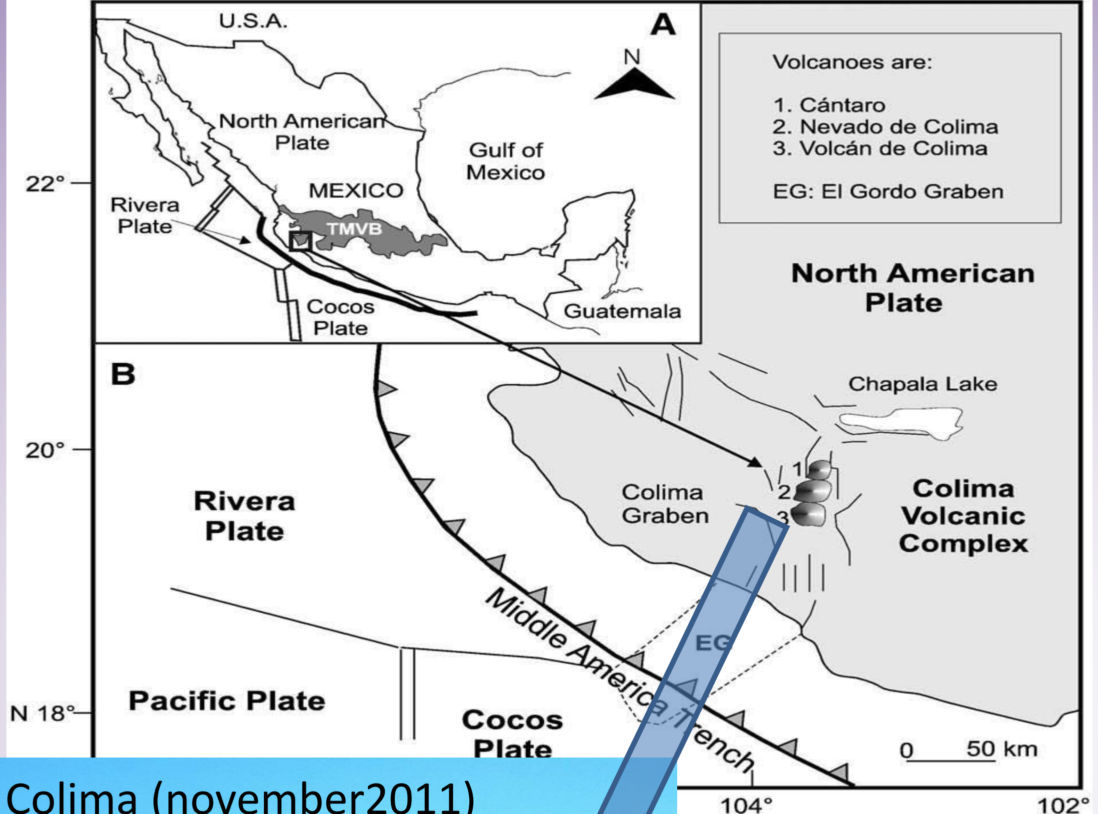

Saucedo et al. 2010

ALEM analysis application to Volcan de Fuego, Colima, MX (Approx 3880 m a.s.l.)

Volcan de fuego Colima, MX

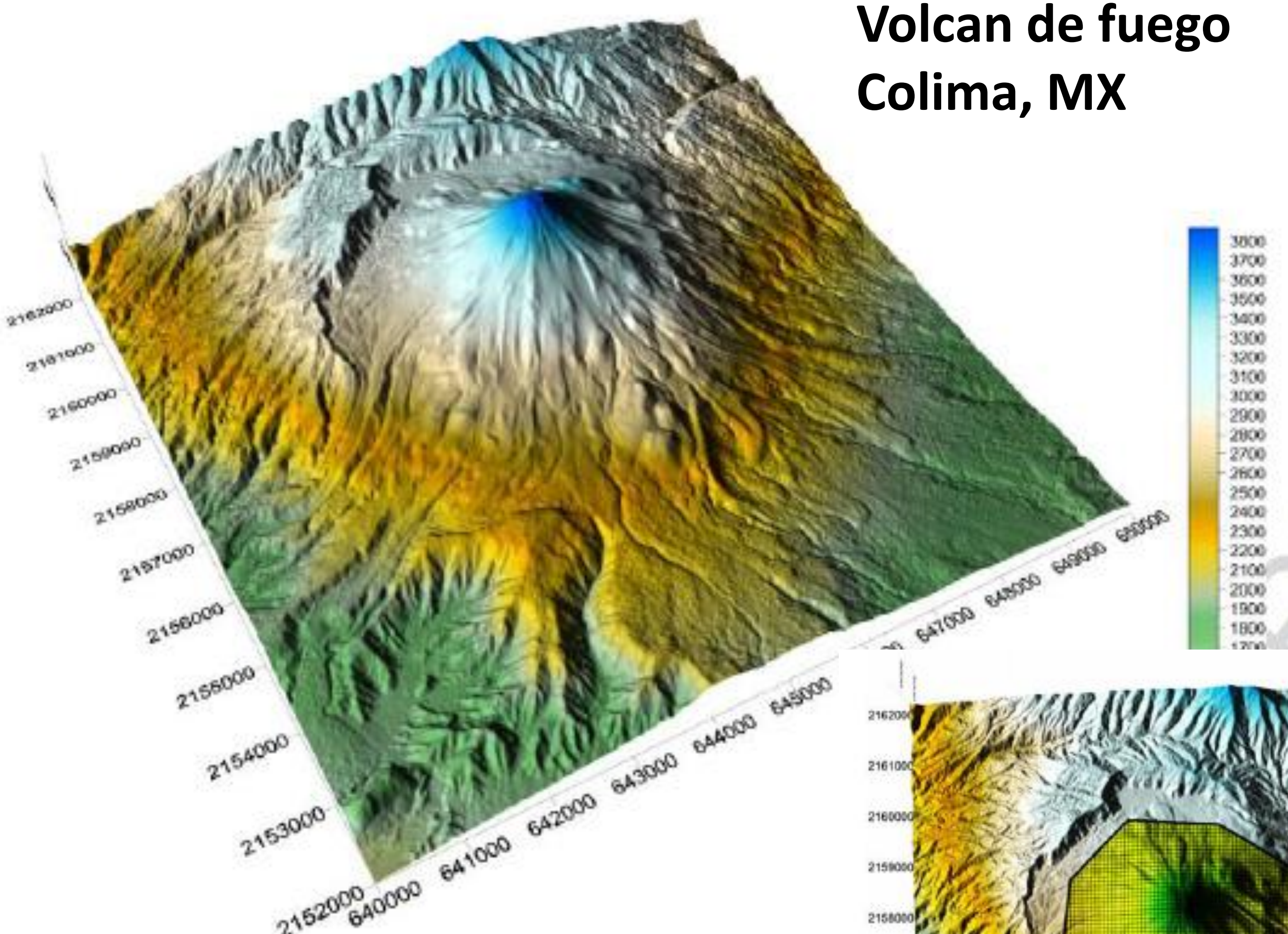

Selected area for analysis

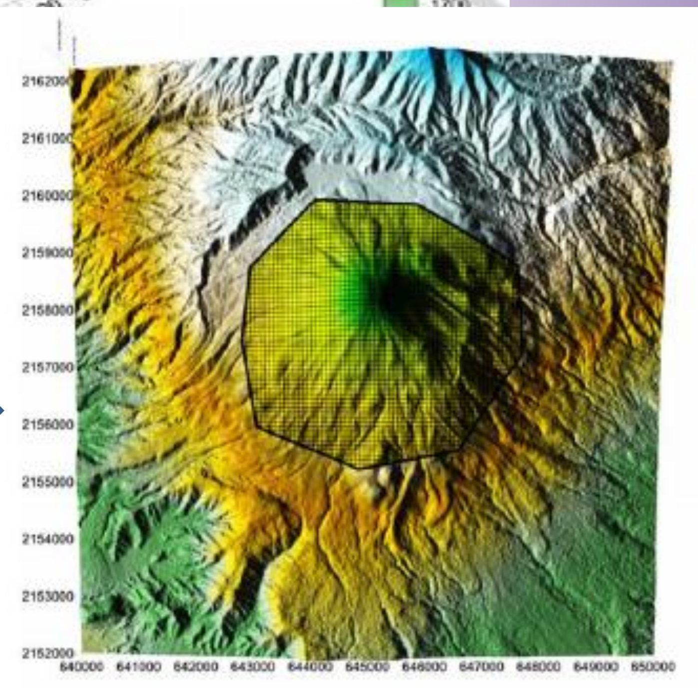

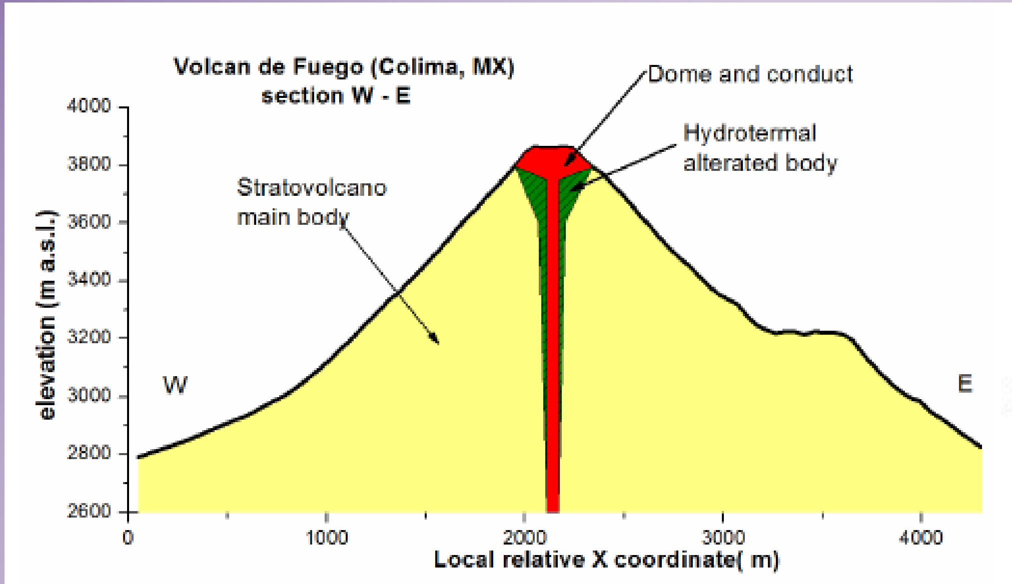
Volcan de Fuego (Colima, MX)
section W - E
Dome and conduct
Hydrotermal
alterated body
Stratovolcano
main body
W
E
elevation (m a.s.l.)
4000
3800
3600
3400
3200
3000
2800
2600
0
1000
2000
3000
4000
Local relative X coordinate(m)

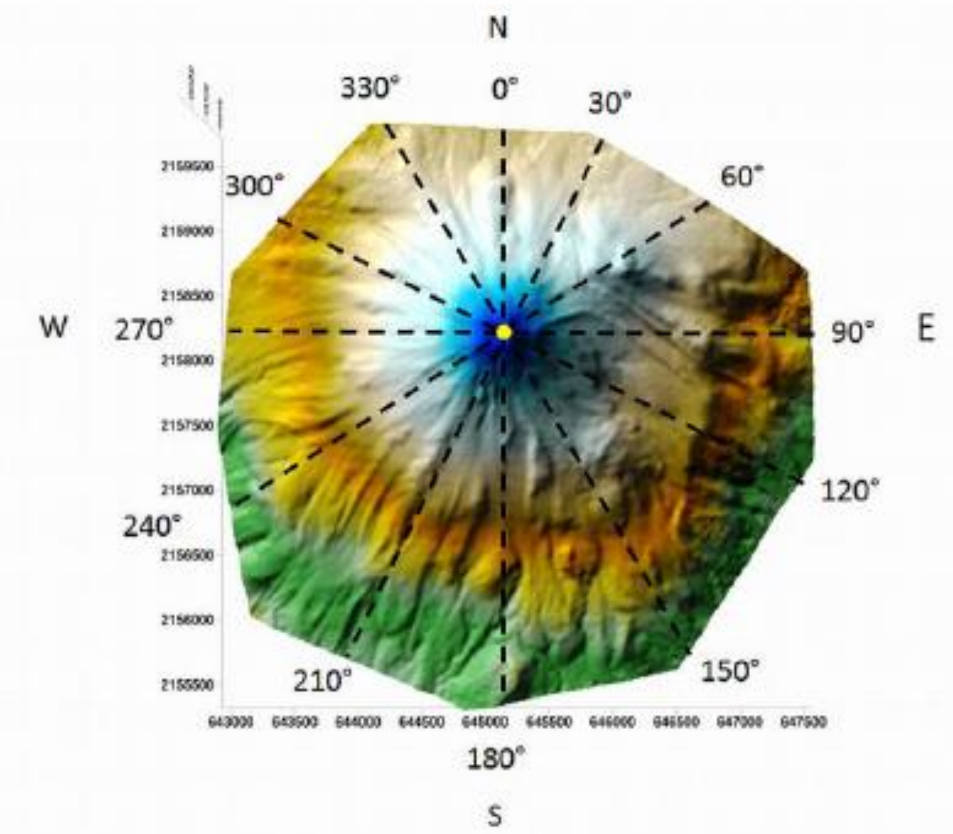
N
330°
0°
30°
300°
60°
W
270°
90°
E
240°
120°
210°
150°
180°
S

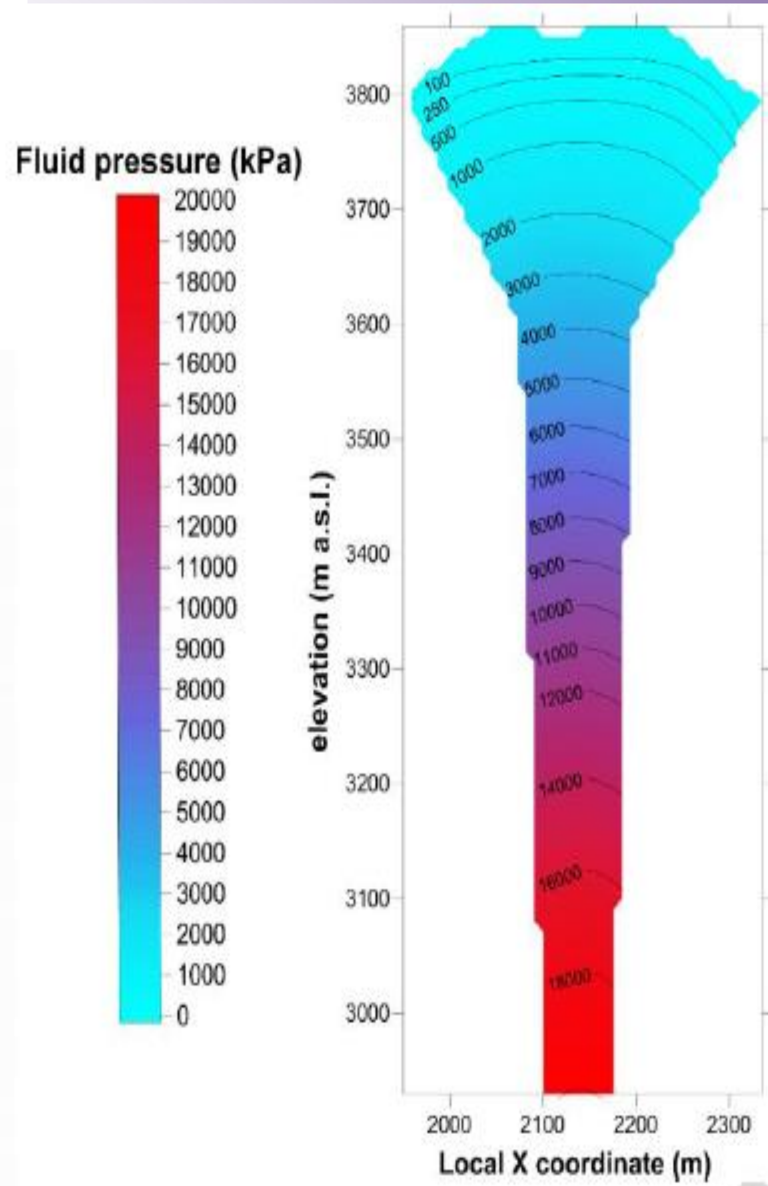
Fluid pressure (kPa)
20000
19000
18000
17000
16000
15000
14000
13000
12000
11000
10000
9000
8000
7000
6000
5000
4000
3000
2000
1000
0
elevation (m a.s.l.)
3800
3700
3600
3500
3400
3300
3200
3100
3000
2000
2100
2200
2300
Local X coordinate (m)

The advanced Limit equilibrium method (ALEM) and Relative instability analysis
Scenarios and mechanical parameters

Shear strength parameterization of main bodies of the stratovolcano following the Hoek and Brown strength criterion (Hoek et al., 2002).

	γ unsaturated unit weight (kN/m³)	γs saturated unit weight (kN/m³)	σl uniaxial compressive strength of intact rock element (MPa)	GSI geological strength index (adimensional)	m_i lithological index (adimensional)	D disturbance factor (adimensional)
Strato volcano main body	24.5	25.0	50	40, (60)*	22	1.0
Hydrothermal altered body	24.0	24.5	40	30, (45)*	22	1.0
Dome and conduct	24.0	24.5	25	20, (30)*	22	1.0

*In parentheses the GSI value for scenario analysis Nos. 2, 3 and 4 (50% increase assumed with respect to GSI of scenario no. 1).

Characteristics of scenario analysis adopted for limit equilibrium analysis.

Scenario no. 1	Description	Notes
1	Geomechanical parameters as in Table 2	No seismic effect
2	Geomechanical parameters as in Table 2 with GSI increase of 50%	No seismic effect
3	The same as scenario 2, but seismic coefficients Kh = 0.2; Kv = 0.1	Seismic effect by LEM pseudostatic analysis
4	The same as scenario 2, but seismic coefficient Kh = 0.25; Kv = 0.125	Seismic effect by LEM pseudostatic analysis

Final results colima with ALEM

L. Borselli et al. / Journal of Volcanology and Geothermal Research 208 (2011) 51–65

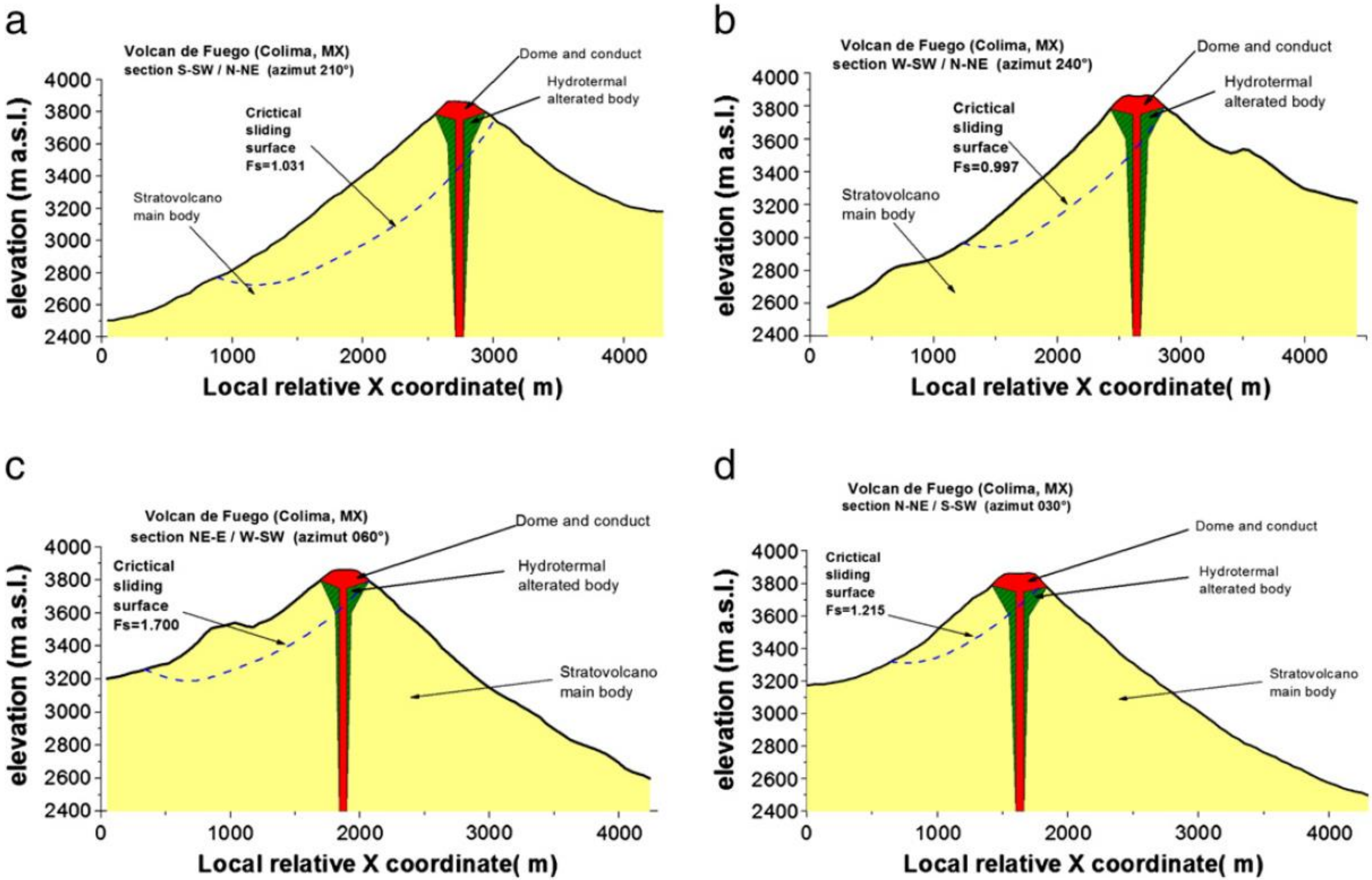

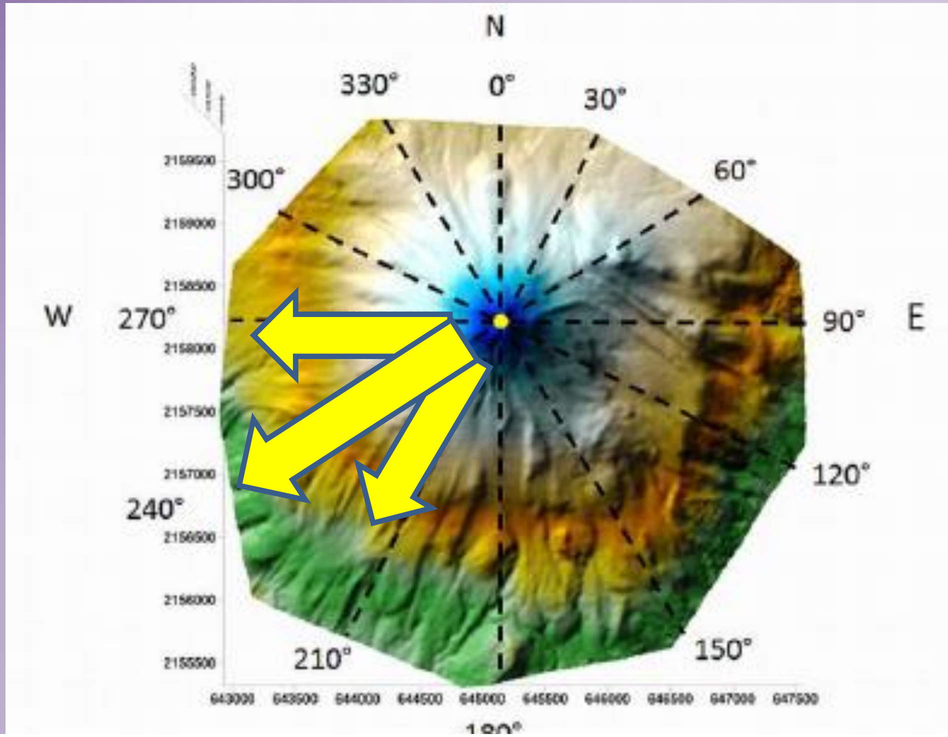

The sector with minimun relative stability is W-SW flank (between 270° and 210°)

The Relative stability index

$$R_{fs_i} = \frac{Fs_i}{Fs_{max}}$$

(Borselli et al. 2011)

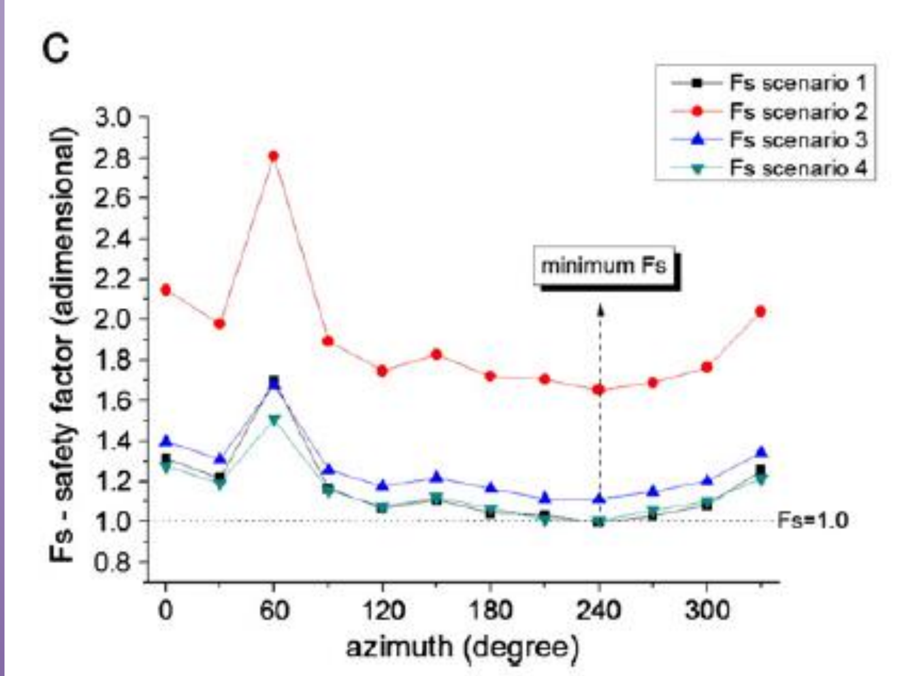

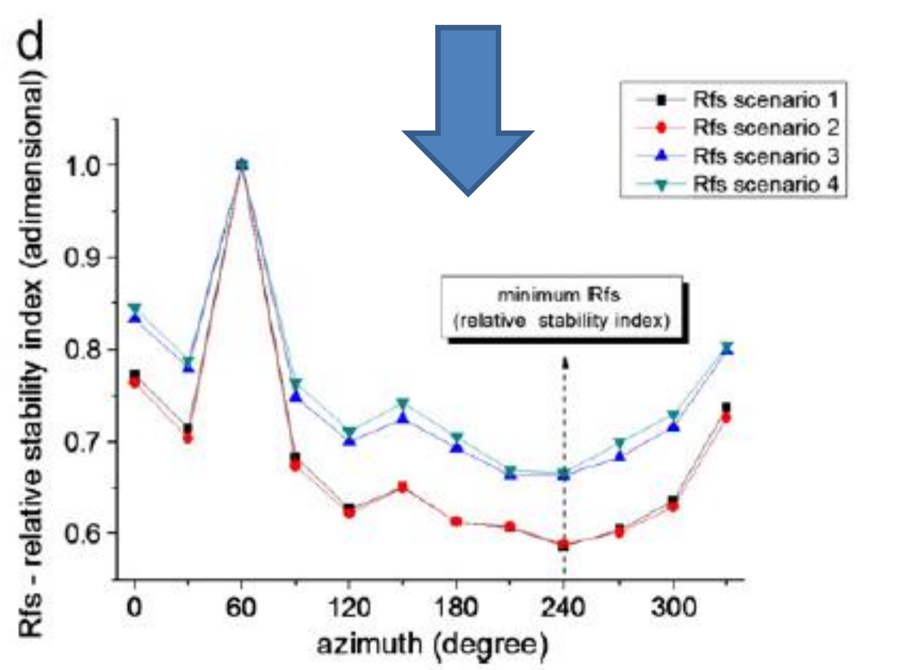

Volcanofit 2.0

WWW. VOLCANOFIT.ORG

$$Z = a\, e^{-\frac{\sqrt{(X-X_0)^2+(Y-Y_0)^2}}{b}} + c \quad \text{if } Z \le Z_1$$

VOLCANOID SURFACE OF REVOLUTION

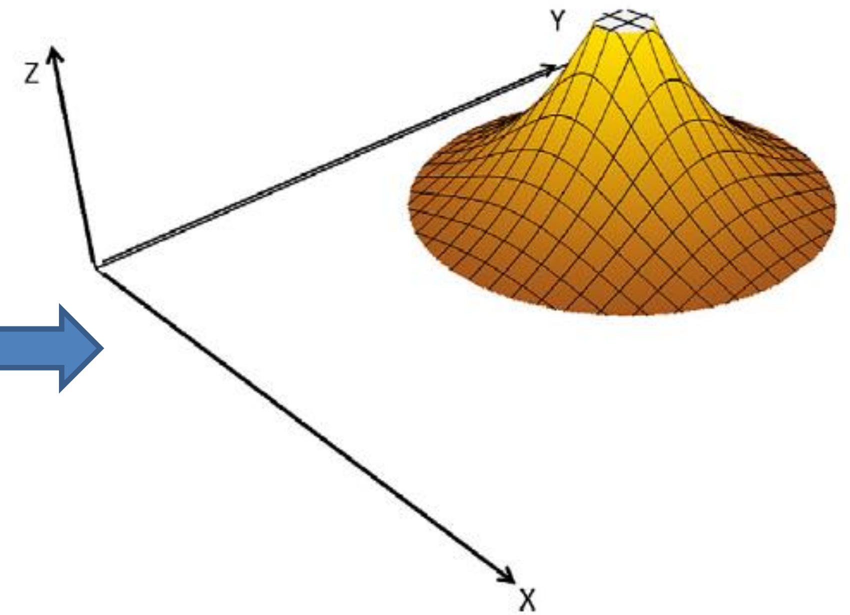

Fig. A.2. Example of volcanoid with constant negative curvature (Eq. (A.5)).

ALTERNATIVE VOLCANOID'S GENERATRIX

$$Z = a \cosh\left(\frac{r-c}{b}\right)$$

for $\forall r < c$ and $a, b, c > 0$.

$$Z = \frac{z_1 - a}{1 + e^{\frac{r-c}{b}}}$$

with $z_1 > a$ and $z_1, a, b, c > 0$.

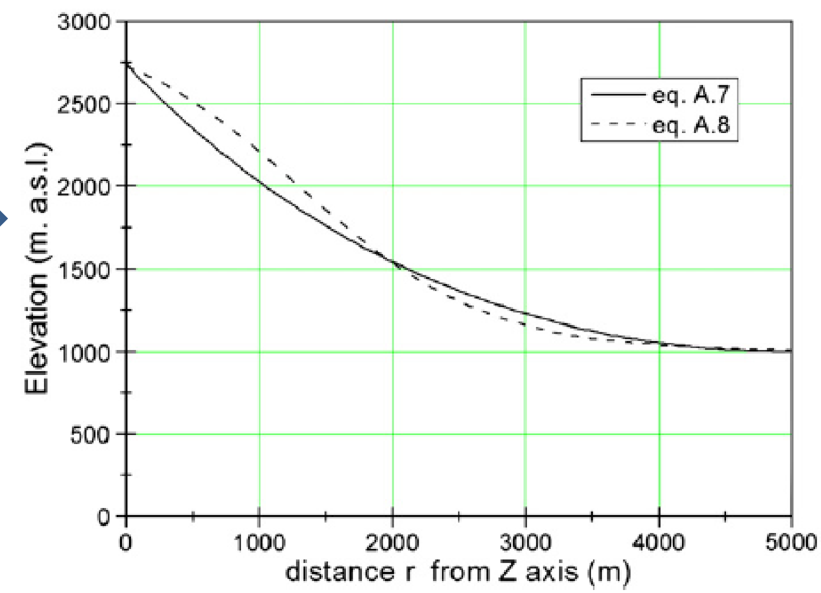

Fig. A.5. Alternative generatrix function of 3D volcanoid.

Colima
Volcanofit 2.0
Result:
Using Negative exponential *Volcanoid*'s generatrix

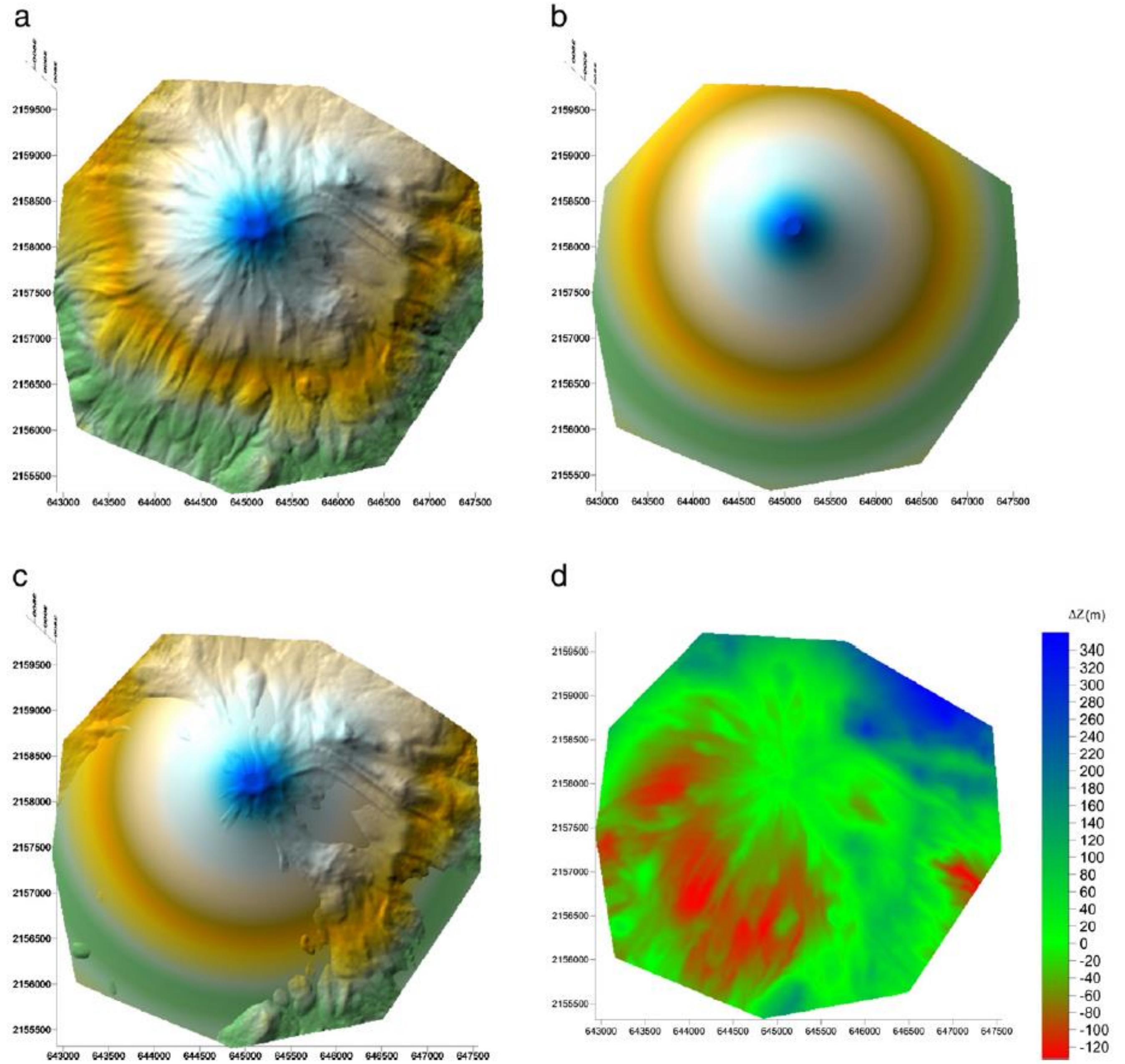

Fig. 7. a) Upper edifice of Colima volcano DEM (2005) b) fitted volcanoid 3D surface Eq. (A.5); c) Upper edifice Colima Volcan de Fuego DEM with overlaid volcanoid Eq. (A.5); d) plot of local deficit (negative values) or surplus (positive values) calculated with Eq. (A.6).

Instituto de Geología

Volcanoid

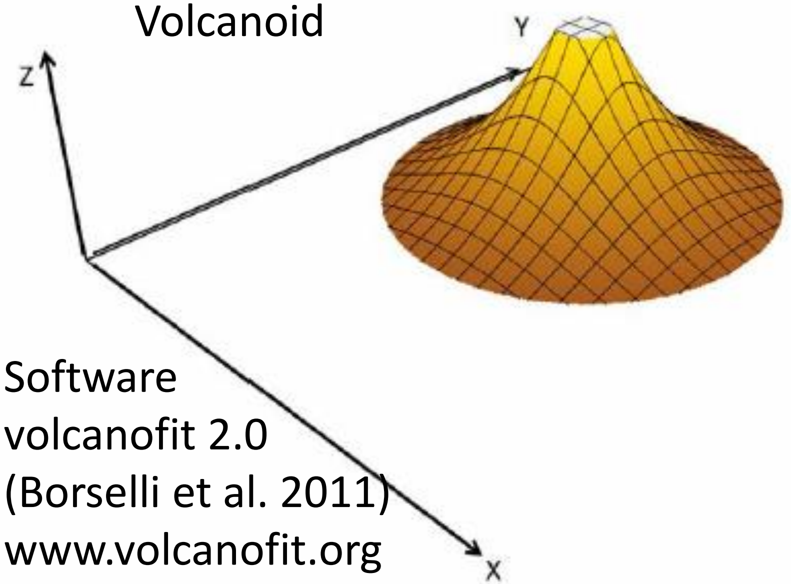

Software
volcanofit 2.0
(Borselli et al. 2011)
www.volcanofit.org

Details overlay DEM and Fitted Volcanoid

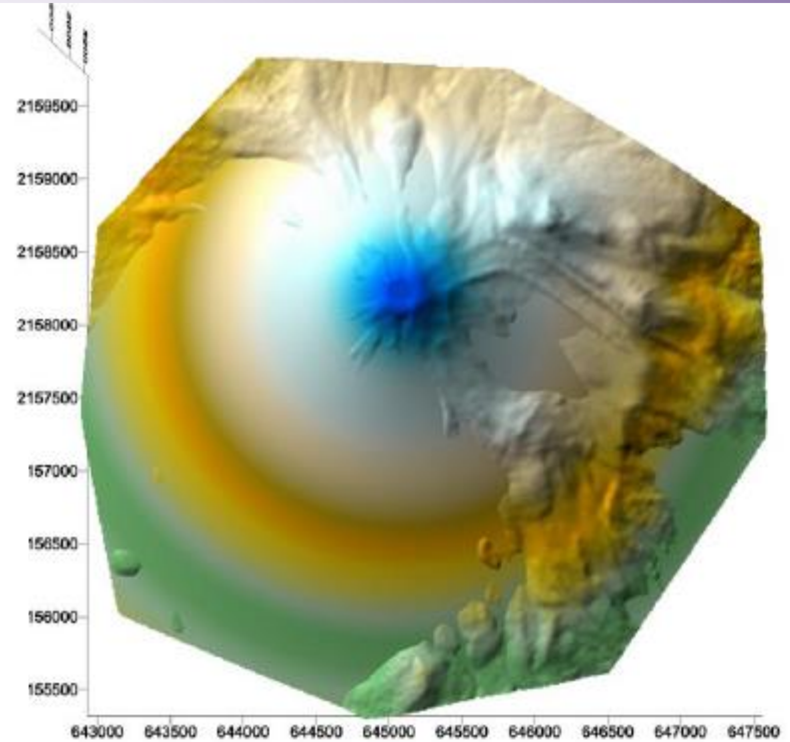

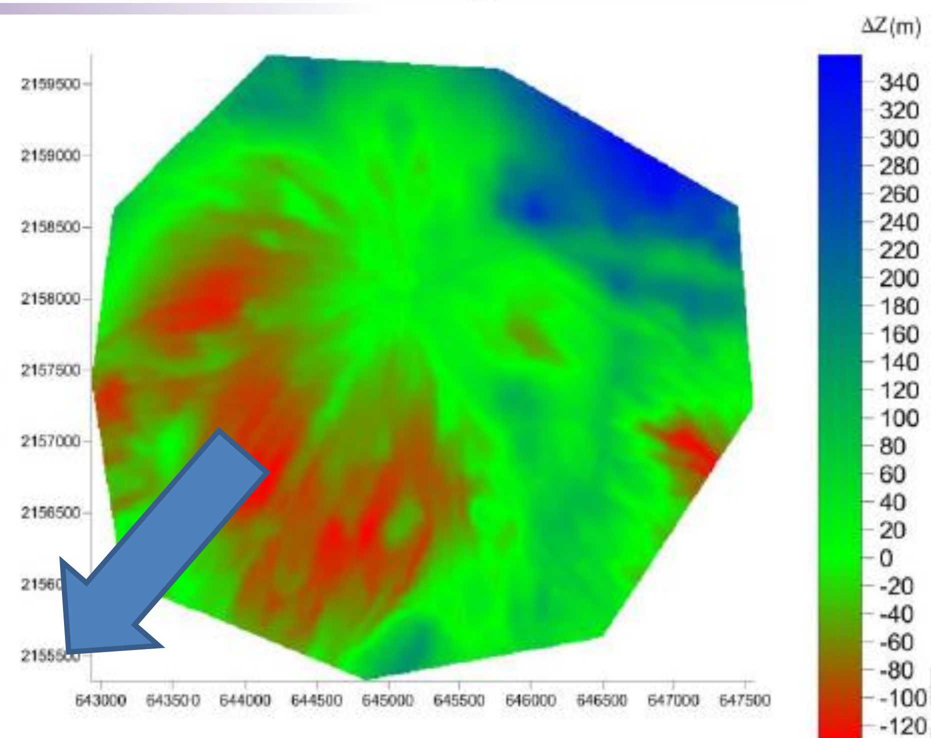

Volume (mass) Deficit
in SW flank

Combined resulys of ALEM (by SSAP 4.0) and VOLCANOFIT2.0

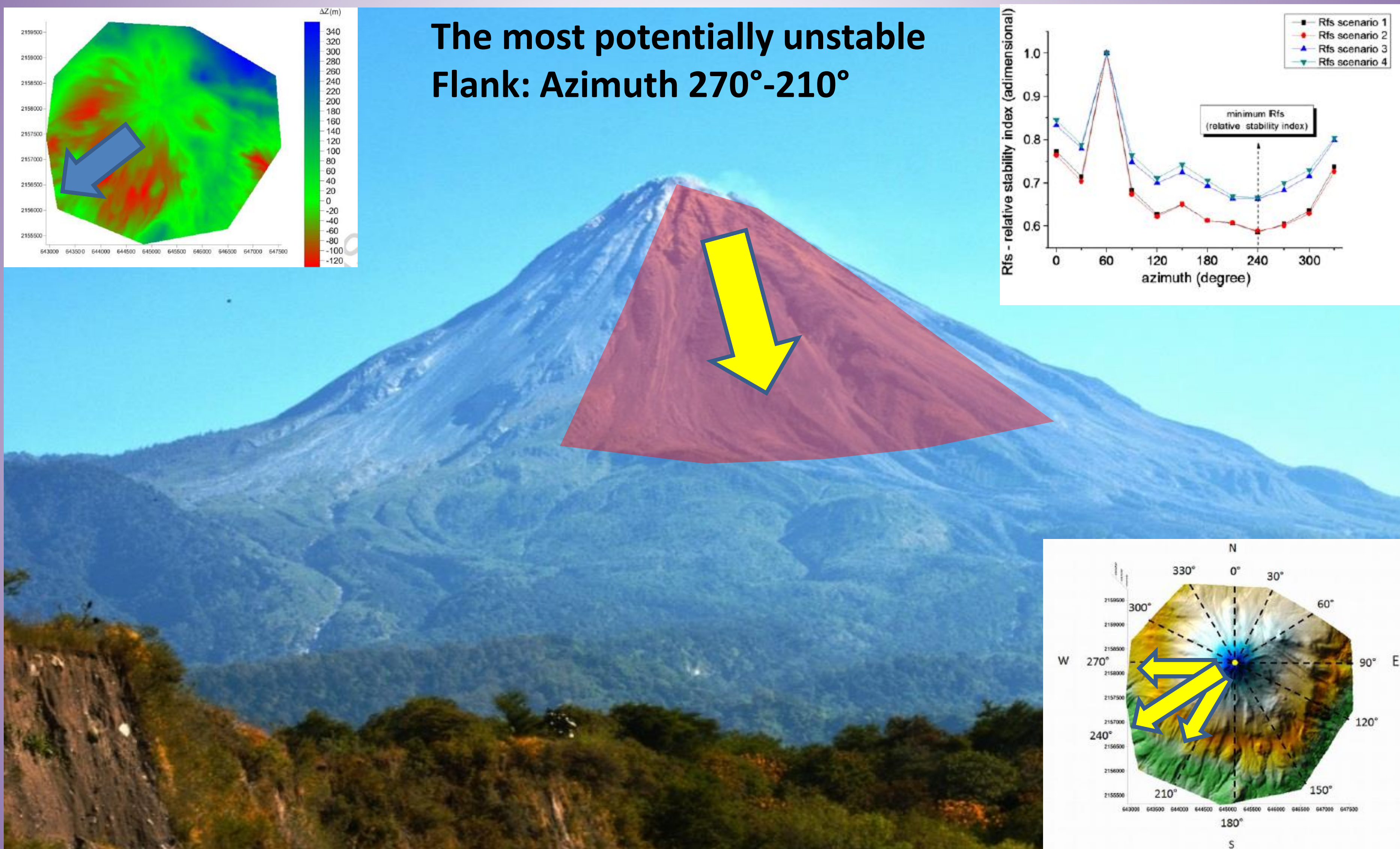

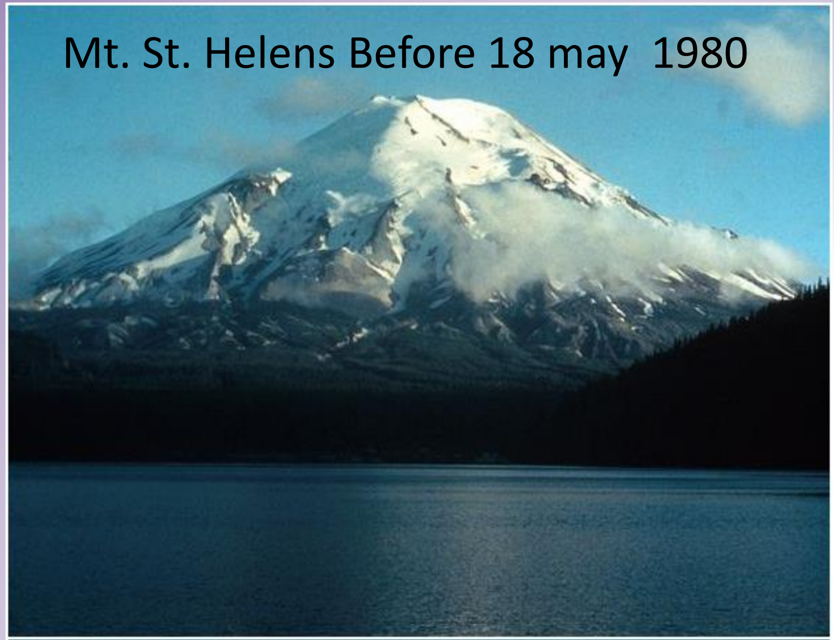

USGS DEM 1979

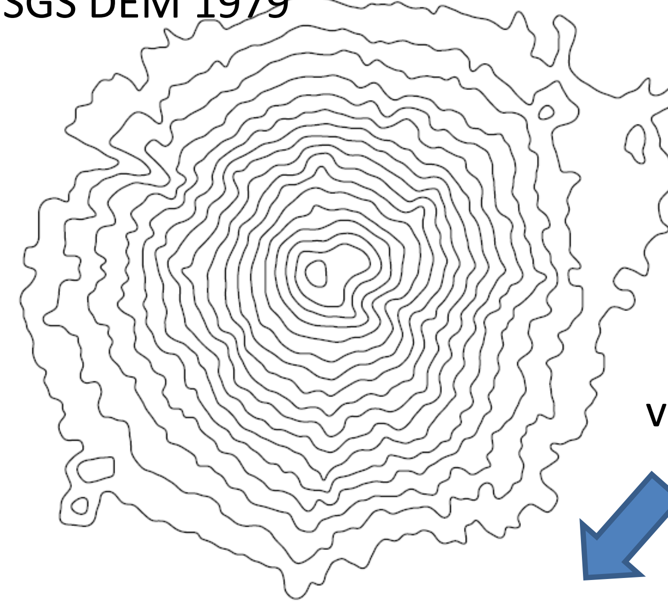

view

USGS DEM after 18 may 1980

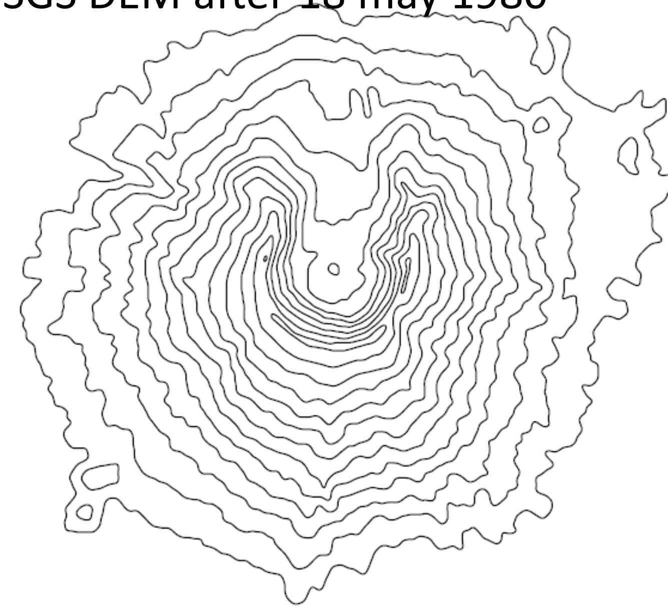

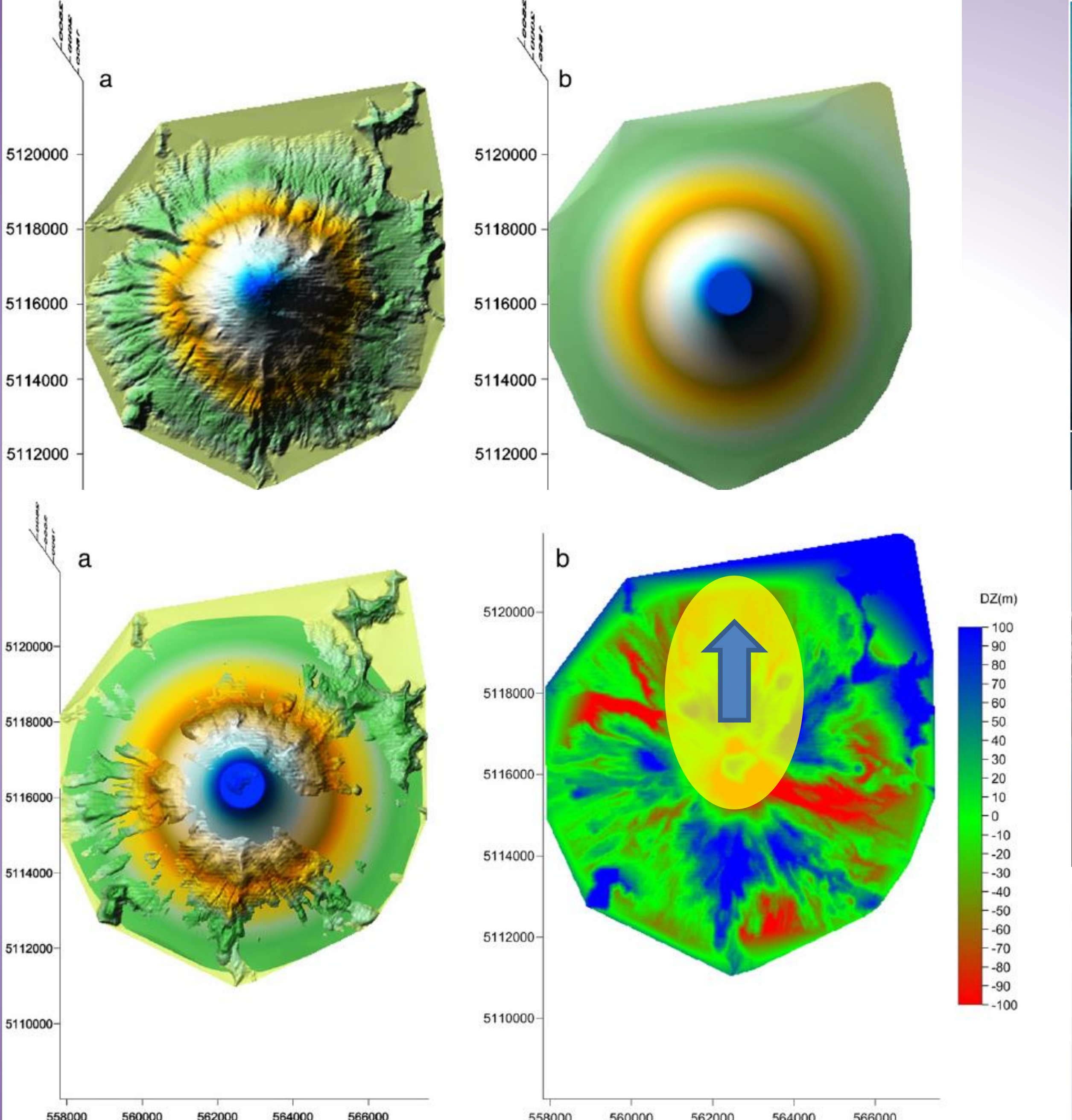

Fig. A.4. a) Pre-eruption 1980 DEM with overlaid volcanoid Eq. (A.5). b) Plot of local deficit (negative values) or surplus (positive values) calculated with Eq. (A.6).

Mt st. helens 1979 DTM
Analysed by **VOLCANOFIT 2.0**
(Borselli et al. 2011)

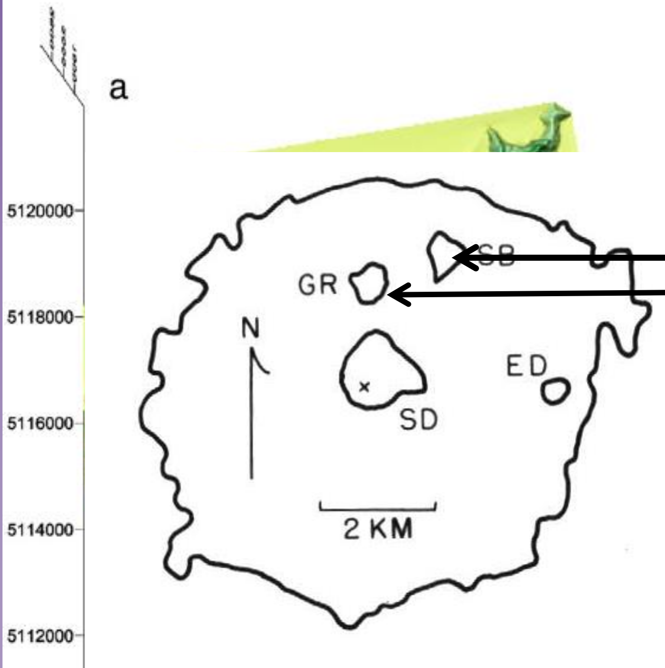

From Hausback and Swanson (1990)

Figure 7 *Northeastern asymmetric distribution of extrusive domes younger than Pine Creek age at Mount St. Helens. Small "**x**" is pre-1980 summit. These domes include east dome (**ED**), Sugar Bowl dome (**SB**), summit dome (**SD**), and Goat Rocks dome (**GR**, removed by 1980 landslide and blast). The 1340-m (4400-ft) contour encircles volcano. Dome outlines from unpublished mapping by C.A. Hopson.*

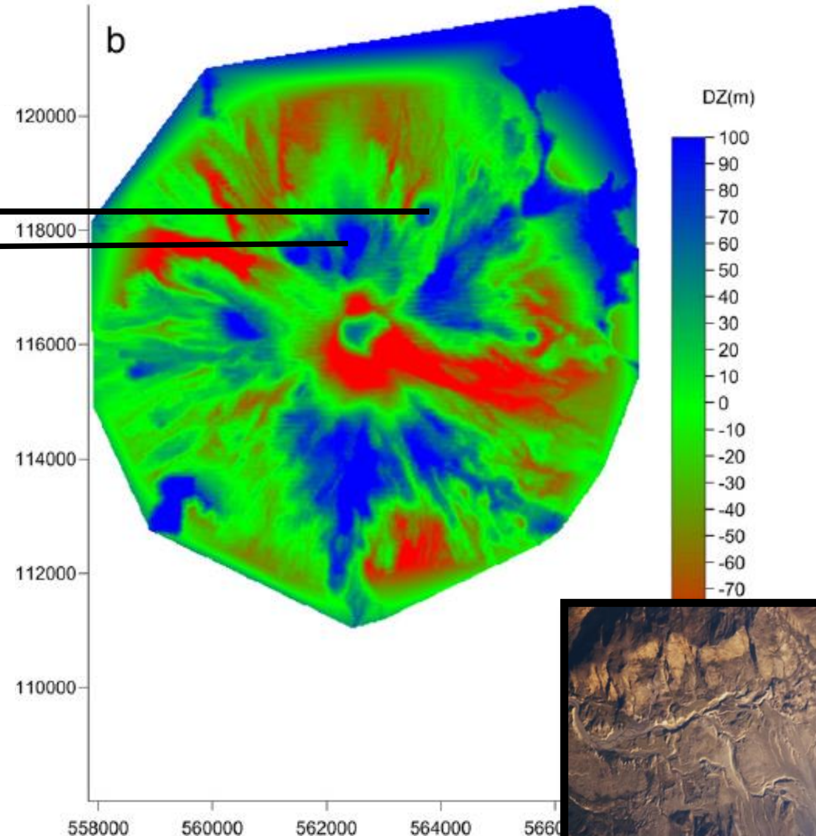

DTM by University of Washington, Earth and Space science, 2010.
http://rocky.ess.washington.edu/data/raster/thirtymeter/mtsthelens/OldMtStHelens.zip

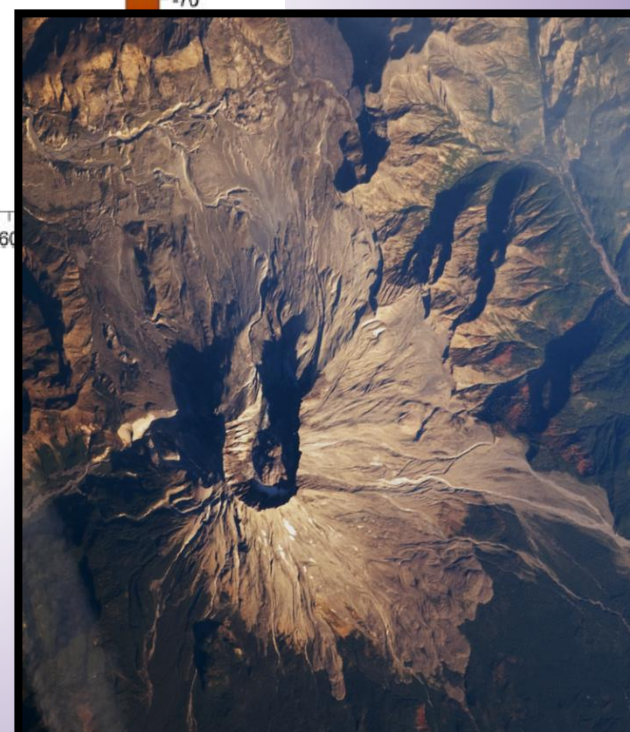

NASA Earth Observatory Image 2009

By (USGS Professional Paper 1250)

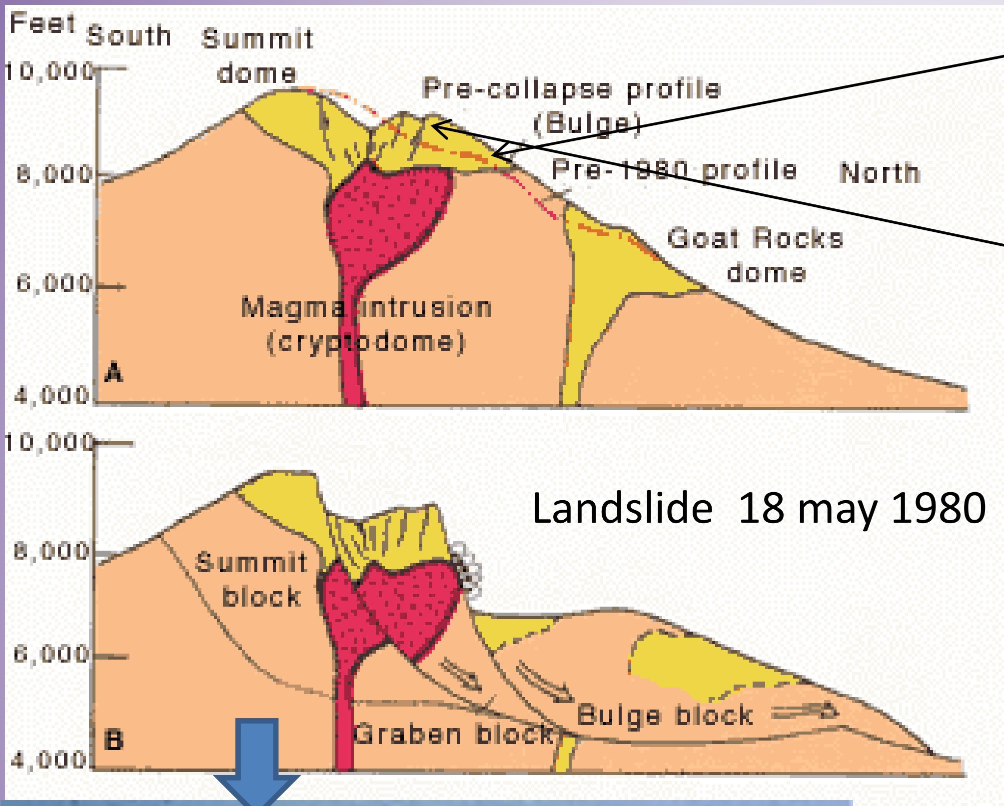

View of the "bulge" on the north face of Mount St. Helens, from a measurement site about 2 miles to the northeast 27 april 1980

http://mountsthelens.com/history-1.html
http://vulcan.wr.usgs.gov/Volcanoes/MSH/Publications/MSHPPF/MSH_past_present_future.html

Los procesos de remoción en masa ocurren a todas las escalas

Los deslizamientos siempre amenazan vidas humanas y infraestructuras sensibles….
casos en Italia

Vernazza 5 terre, Italia
despues el evento del 25
octubre 2011
520 mm de lluvia en 7 horas

Estructuras de conservación del suelos y Mini-taludes de Terrazas pueden ser inestables por errores de diseño, falta de mantenimiento u cambio climático (incremento de frequencia de lluvias extremas).

5 terre, Italia 25 octubre 2011 – 520 mm en 7 horas

Un Herramienta software Freeware de modelado de inestabilidad , para el diseño de obras de estabilización y evaluación de condiciones de peligro

El software SSAP 4.7.2 (1991,2016)

WWW.SSAP.EU

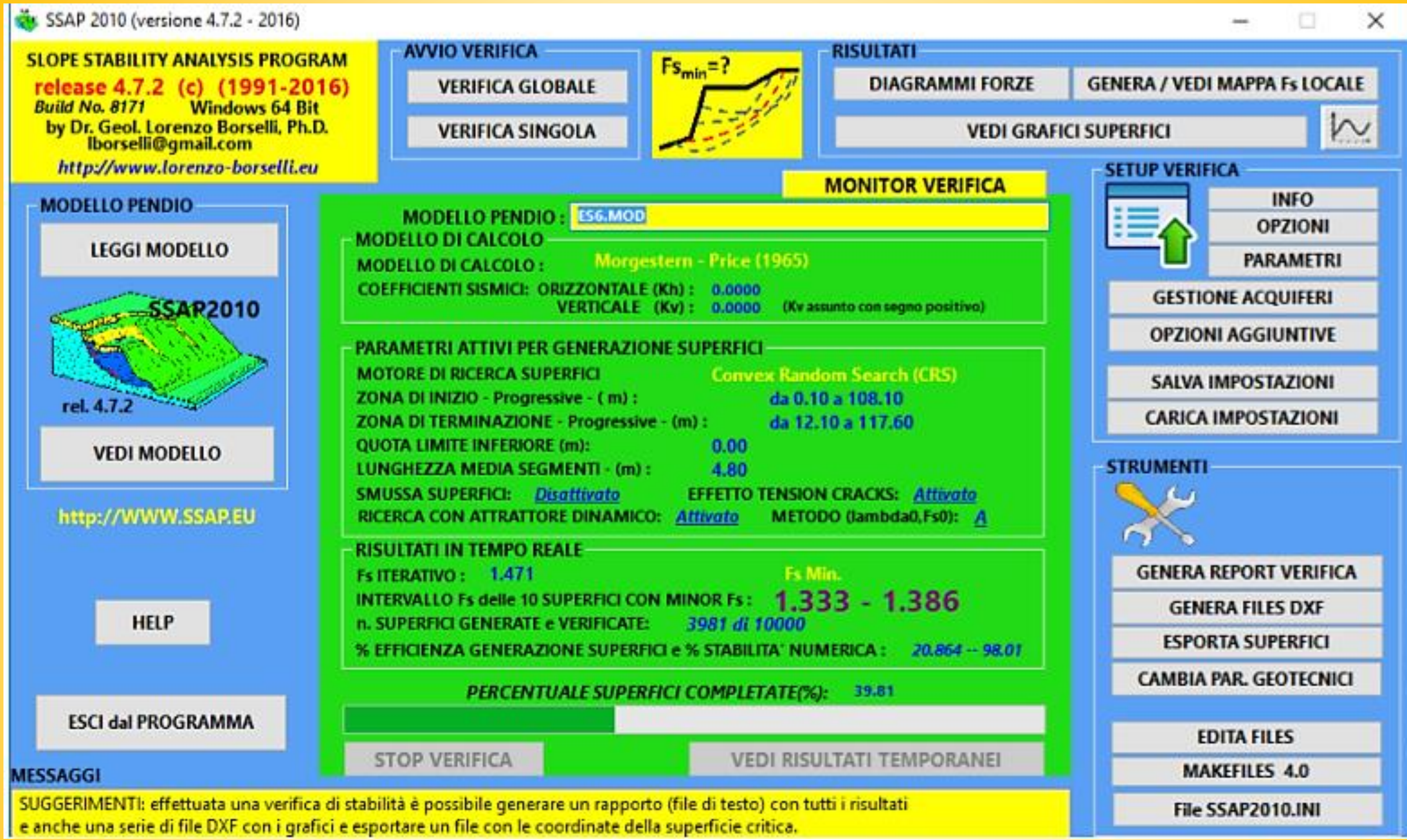

SSAP 4.7.2 - WWW.SSAP.EU

Software totalmente freeware , para investigadores, ingenieros, estudiantes
Interfaz grafica WIN 10

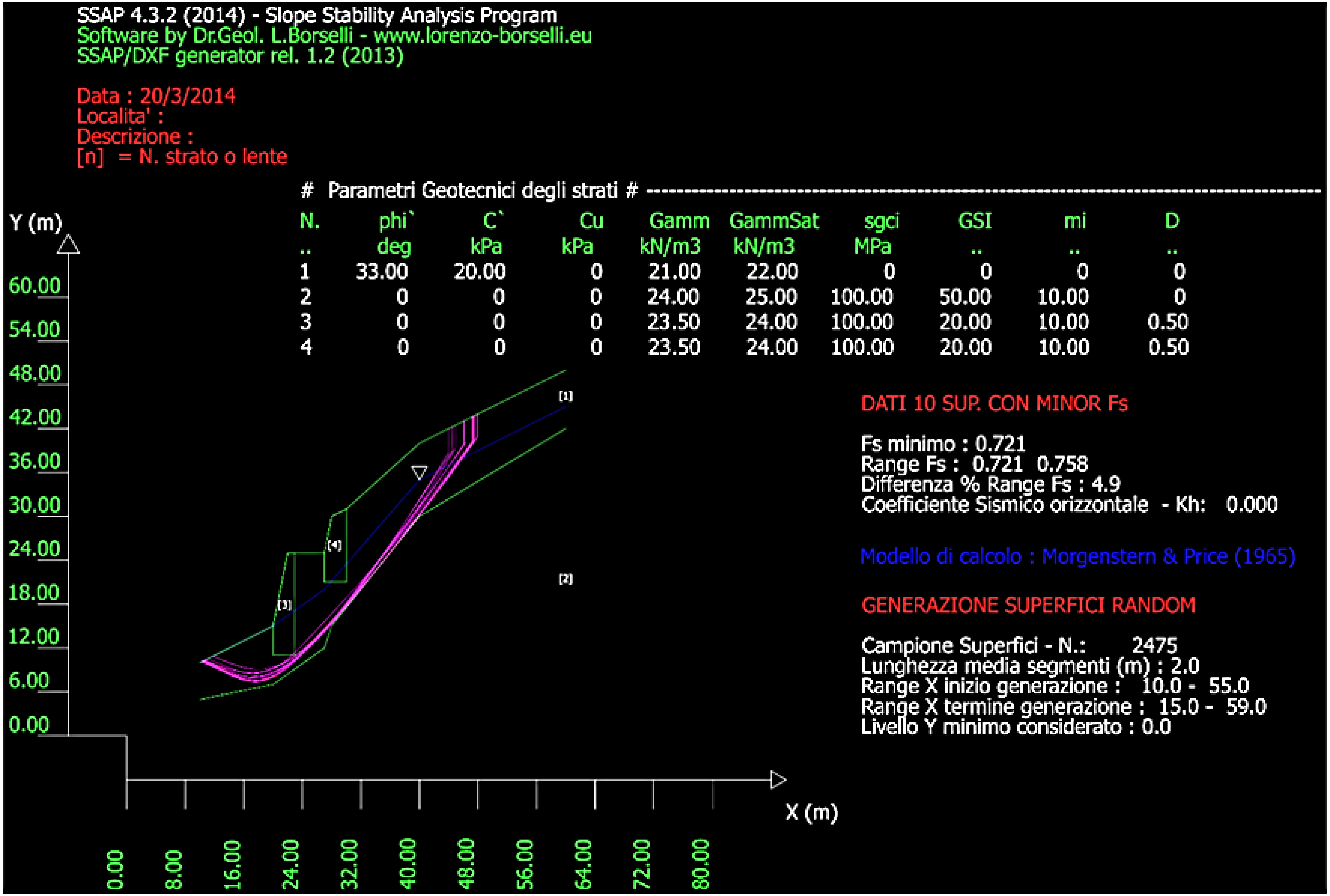

Combinación de criterio de ruptura en un mismo talud

- Mohr –Coulomb cobertura colluvial de suelos residuales
- Hoek (2002,2006) – macizo rocosos fracturados y terrazas con megabloques

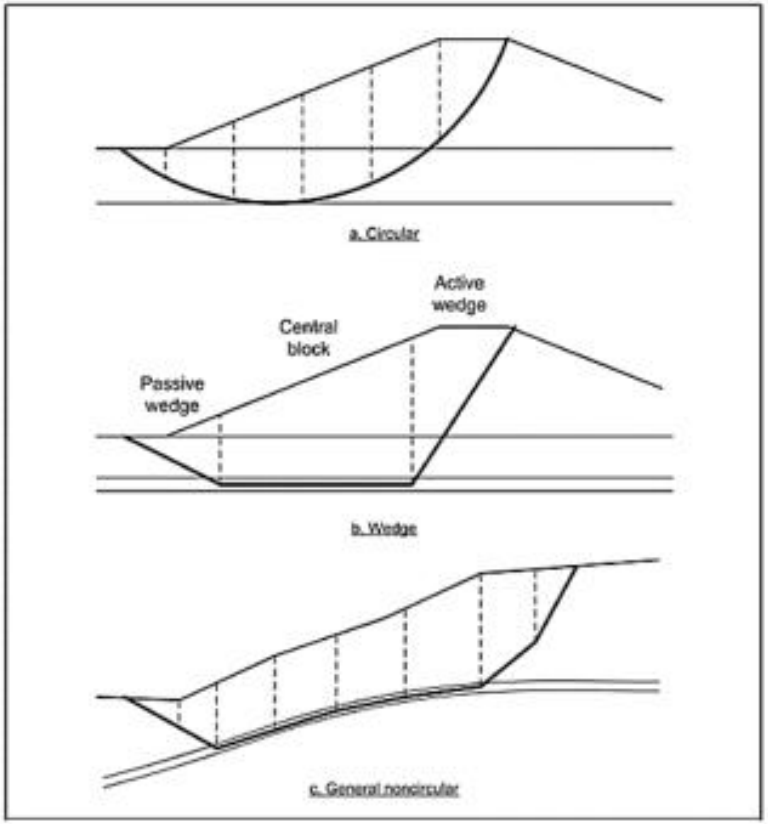

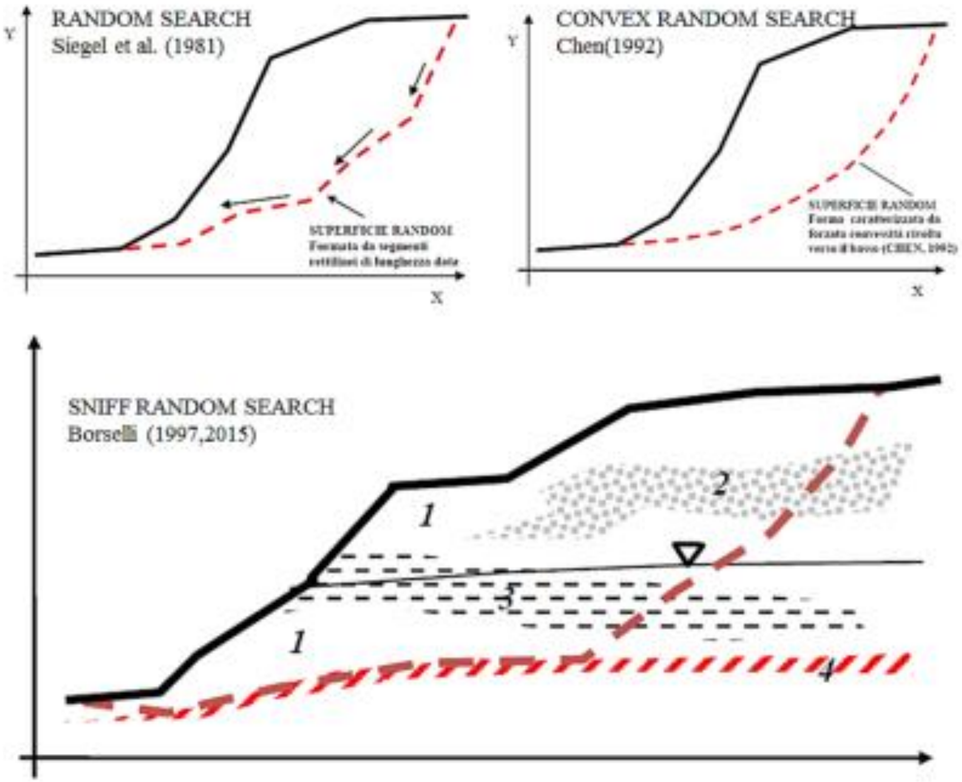

Generacion automática de superficies de forma general
Con metdod monte carlo y sniff search

Modelado de efecto
Estabilizante de un talud inestable
Con lineas de palos pilotes en SSAP 4.7.2

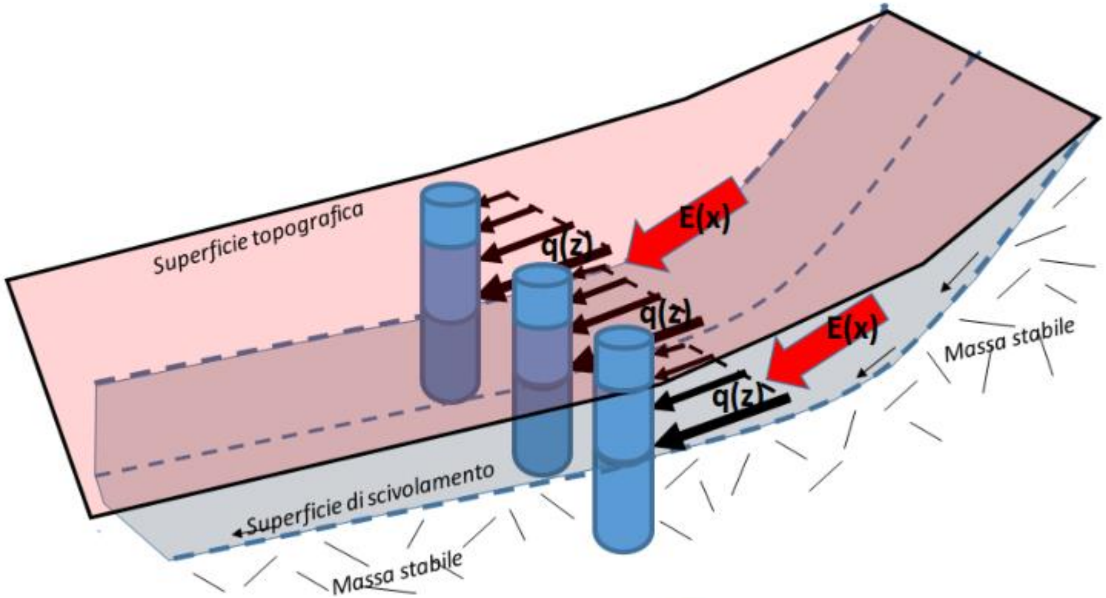

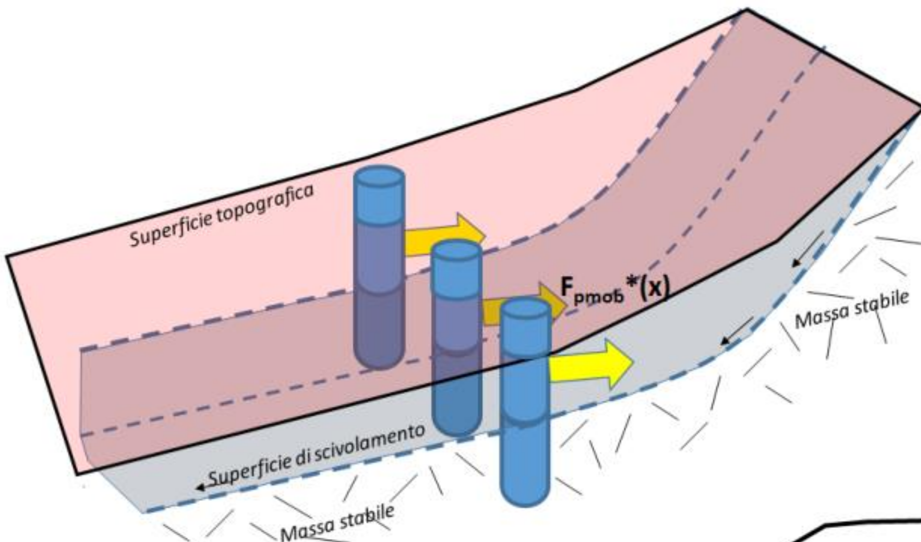

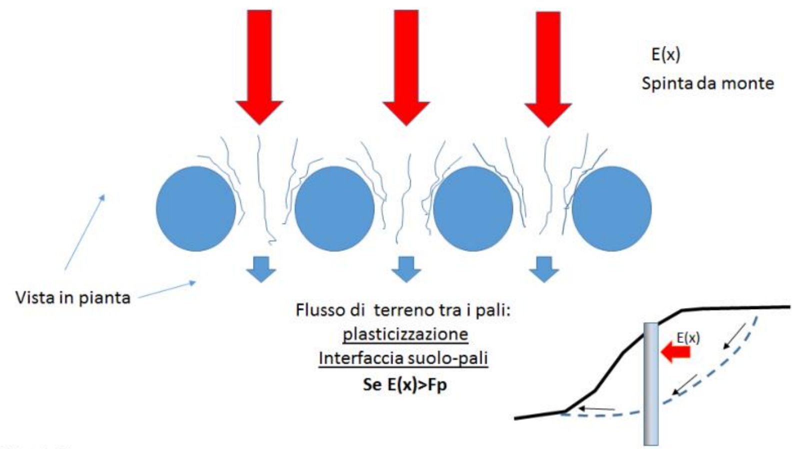

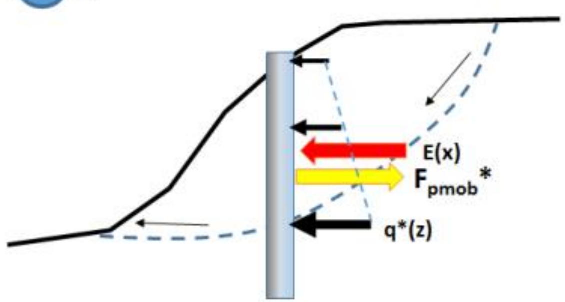

Otras estructuras de contención
Anclajes, reinforced earths, geogrids
Muros, gabions.. Etc.

Mapas en colores
Con valores de FS locales
Y zonas de plasticizacion
Posibles

Efectos sísmicos

Metods de calculo
riguros LEM:
Spencer,
Sarma I y II, Janbu riguroso
Morgestern & Price
Chen & Morgestern

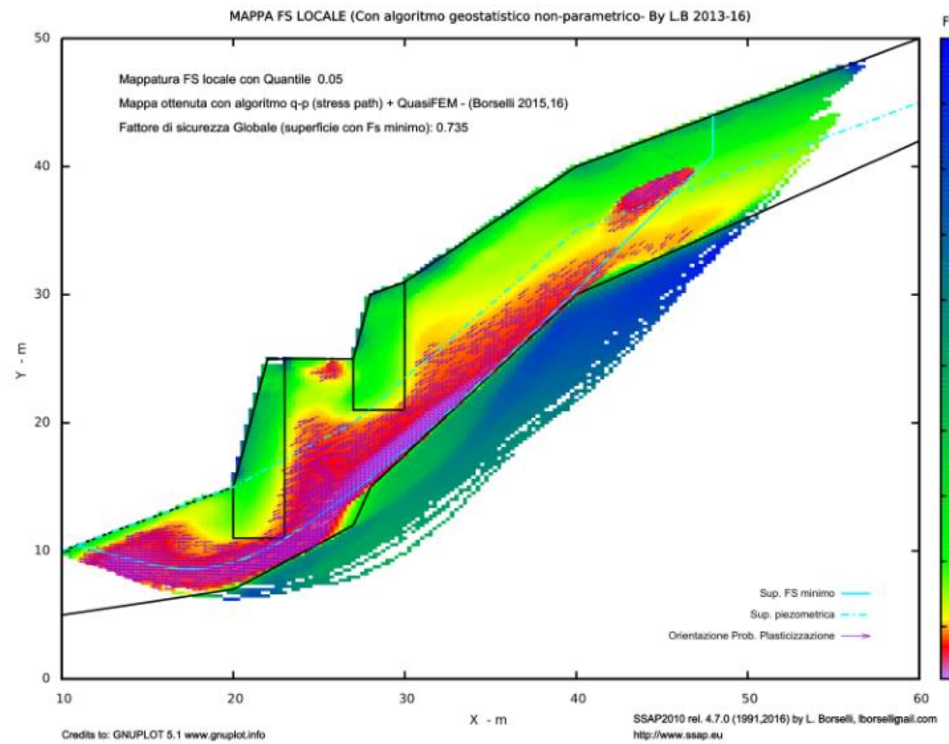

Fig. 2.49

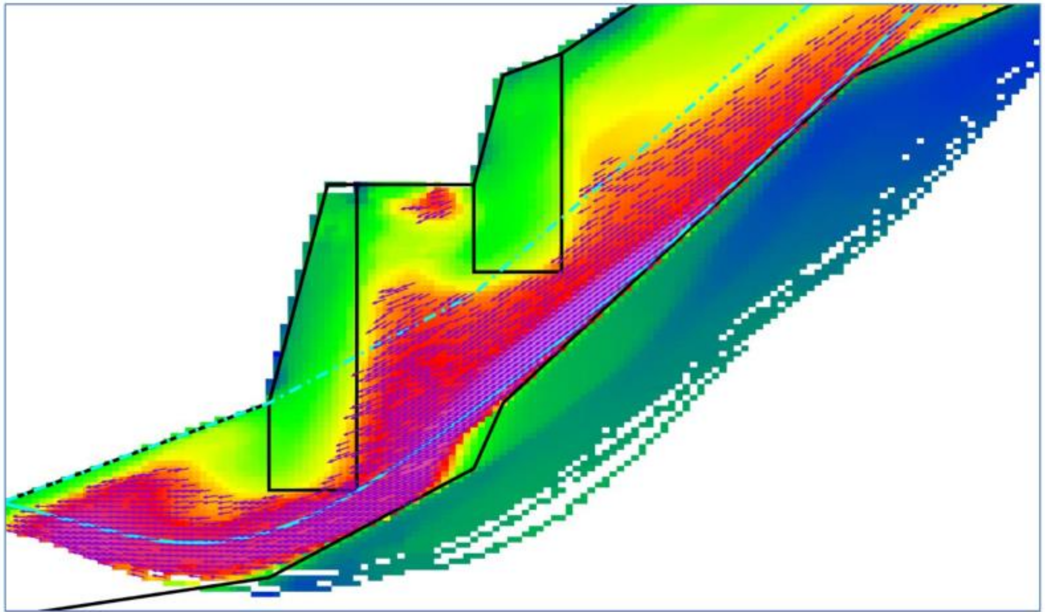

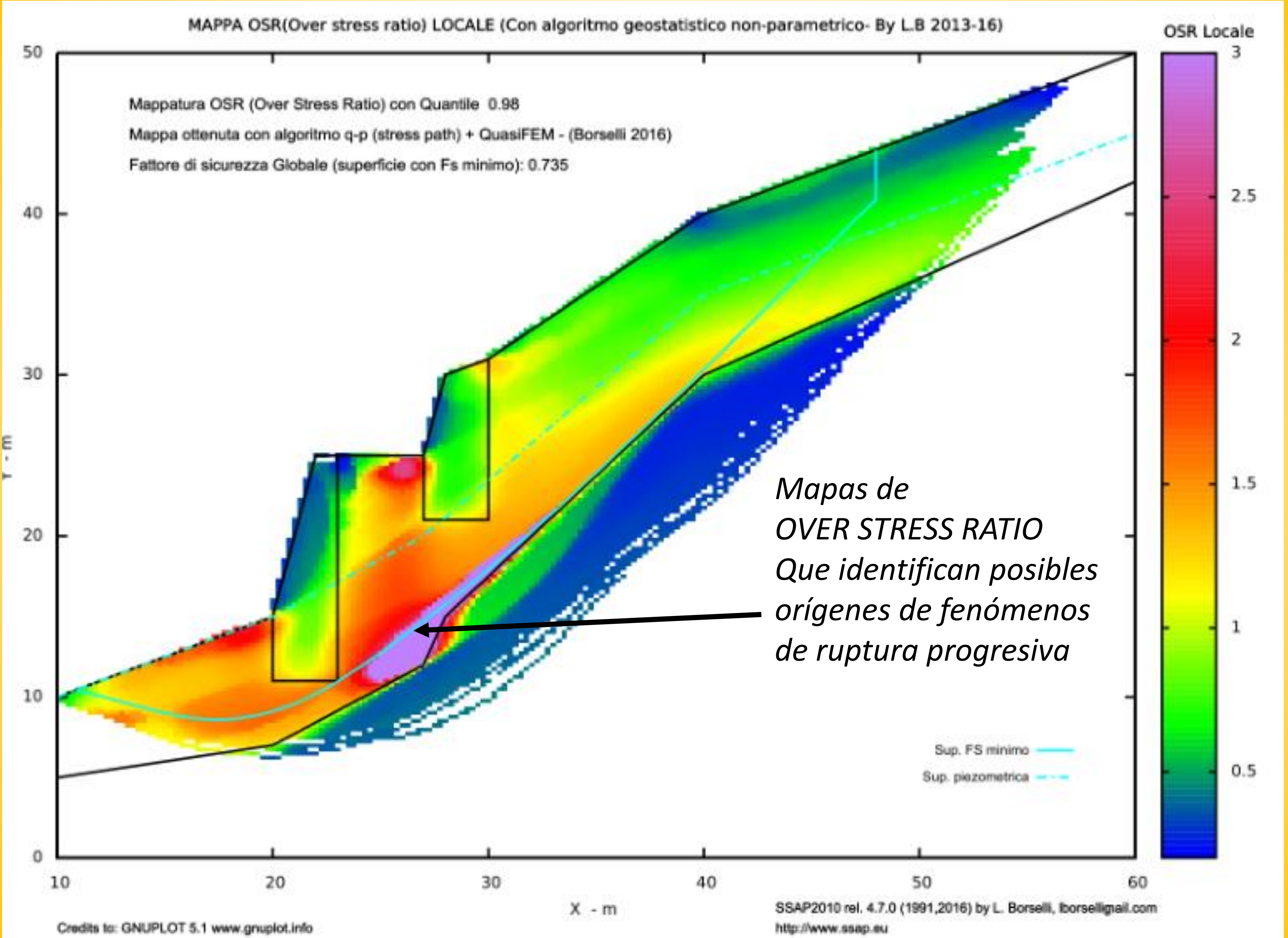

Mapas de OVER STRESS RATIO Que identifican posibles orígenes de fenómenos de ruptura progresiva

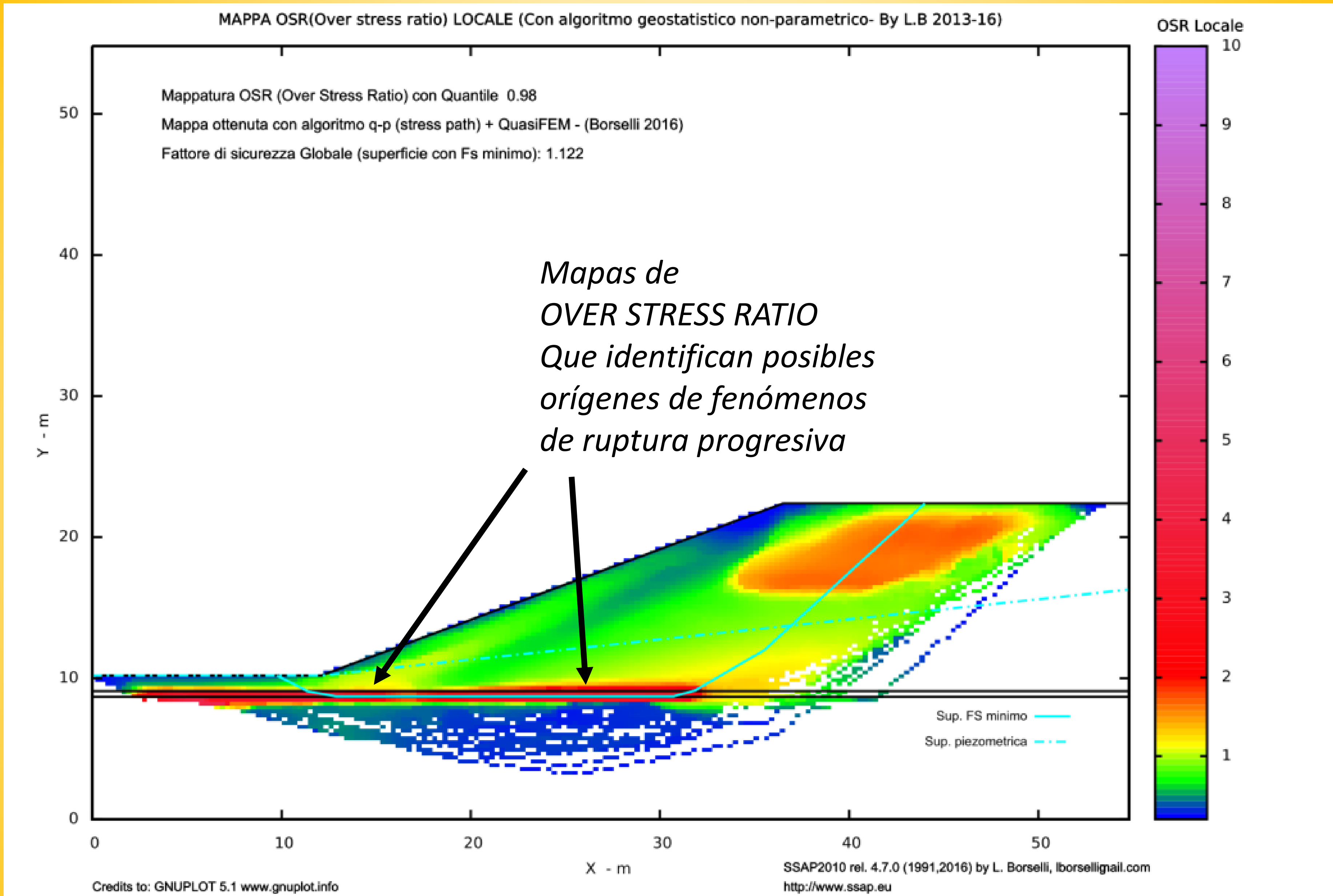

Mapas de
OVER STRESS RATIO

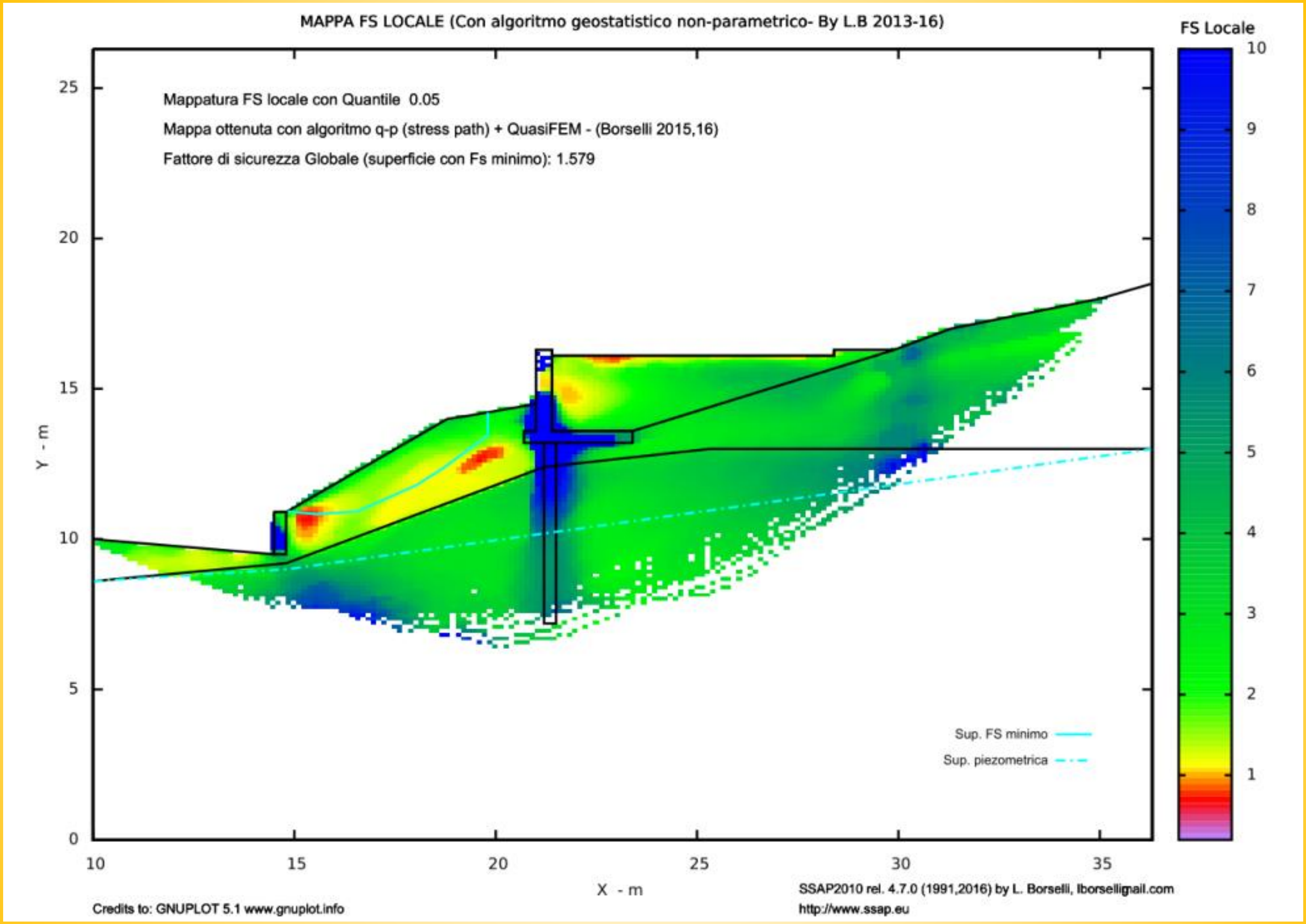

Estucturas composita de contencion

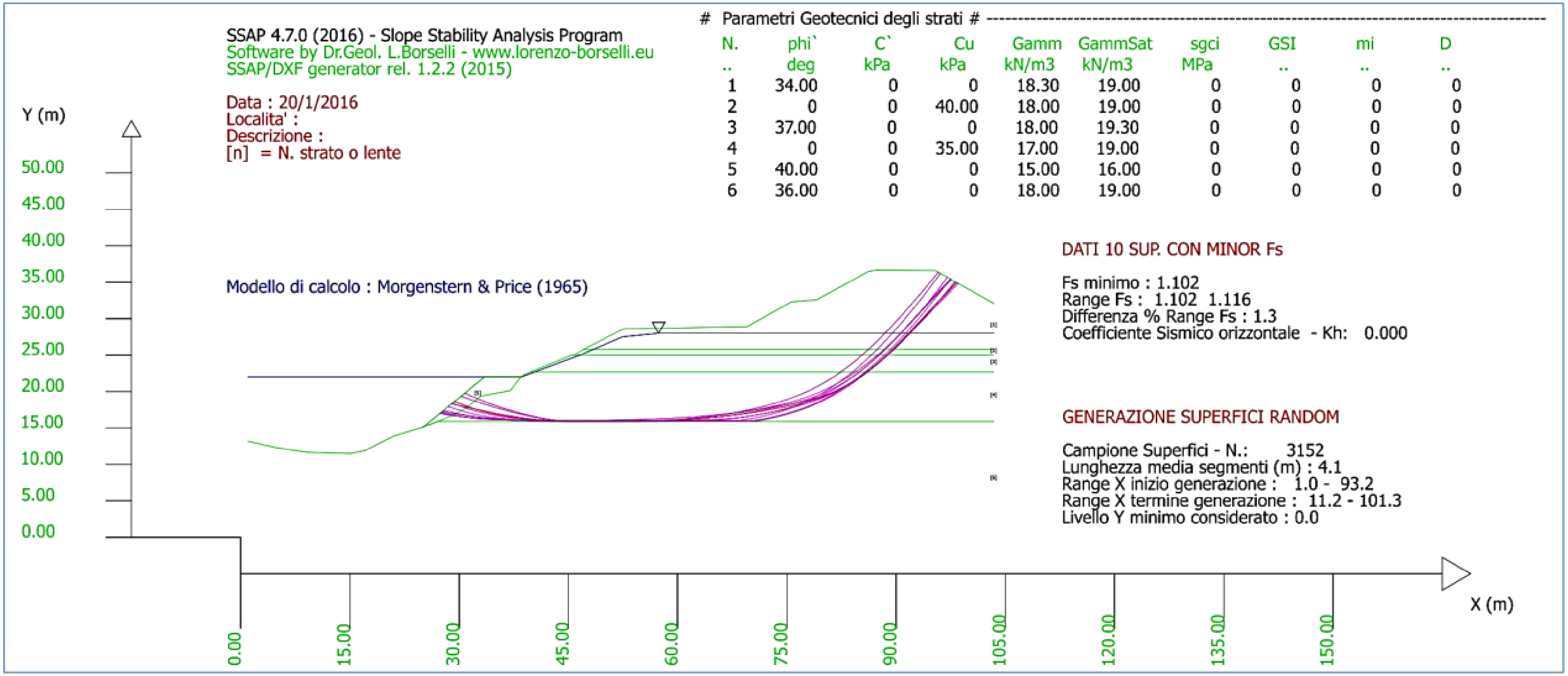

Verifica Estructuras de dique en el Rio Po

Verifica Estructuras de dique en el Rio Po

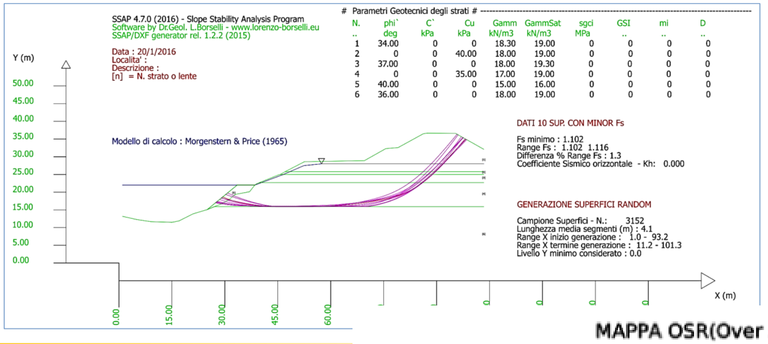

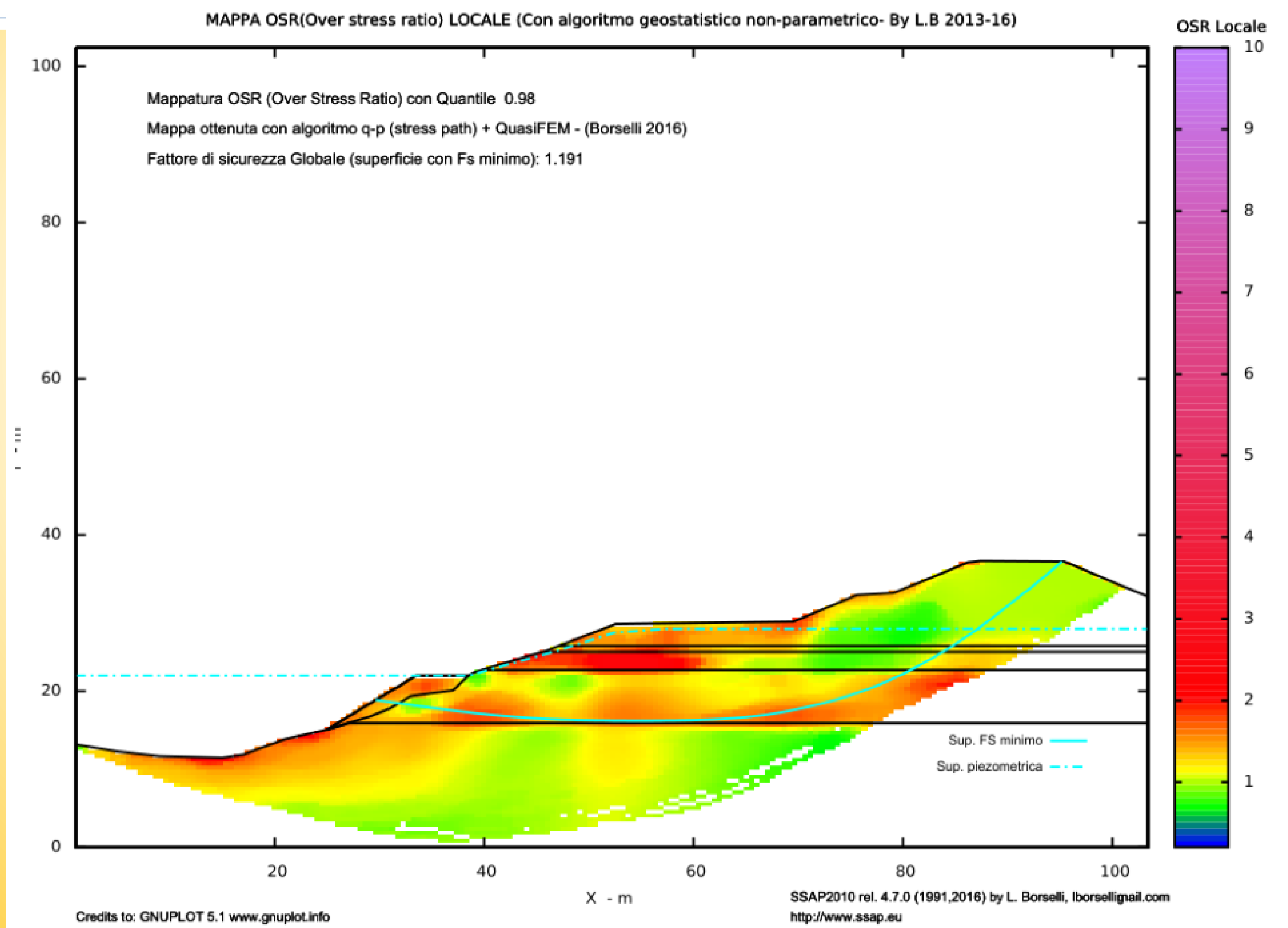

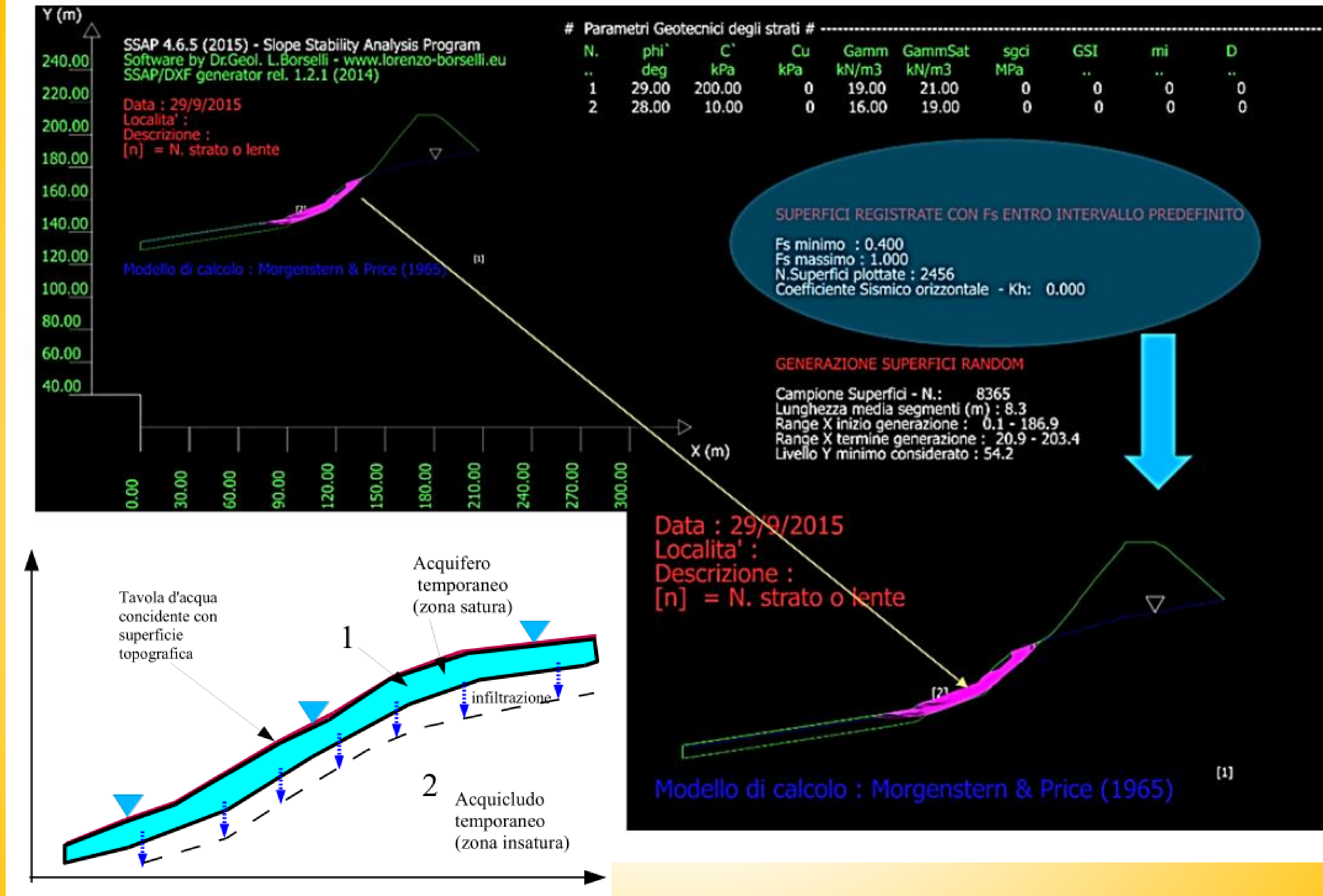

Acuifero temporal colgado, que ha disparado mudflow , Sicilia Italia 2014

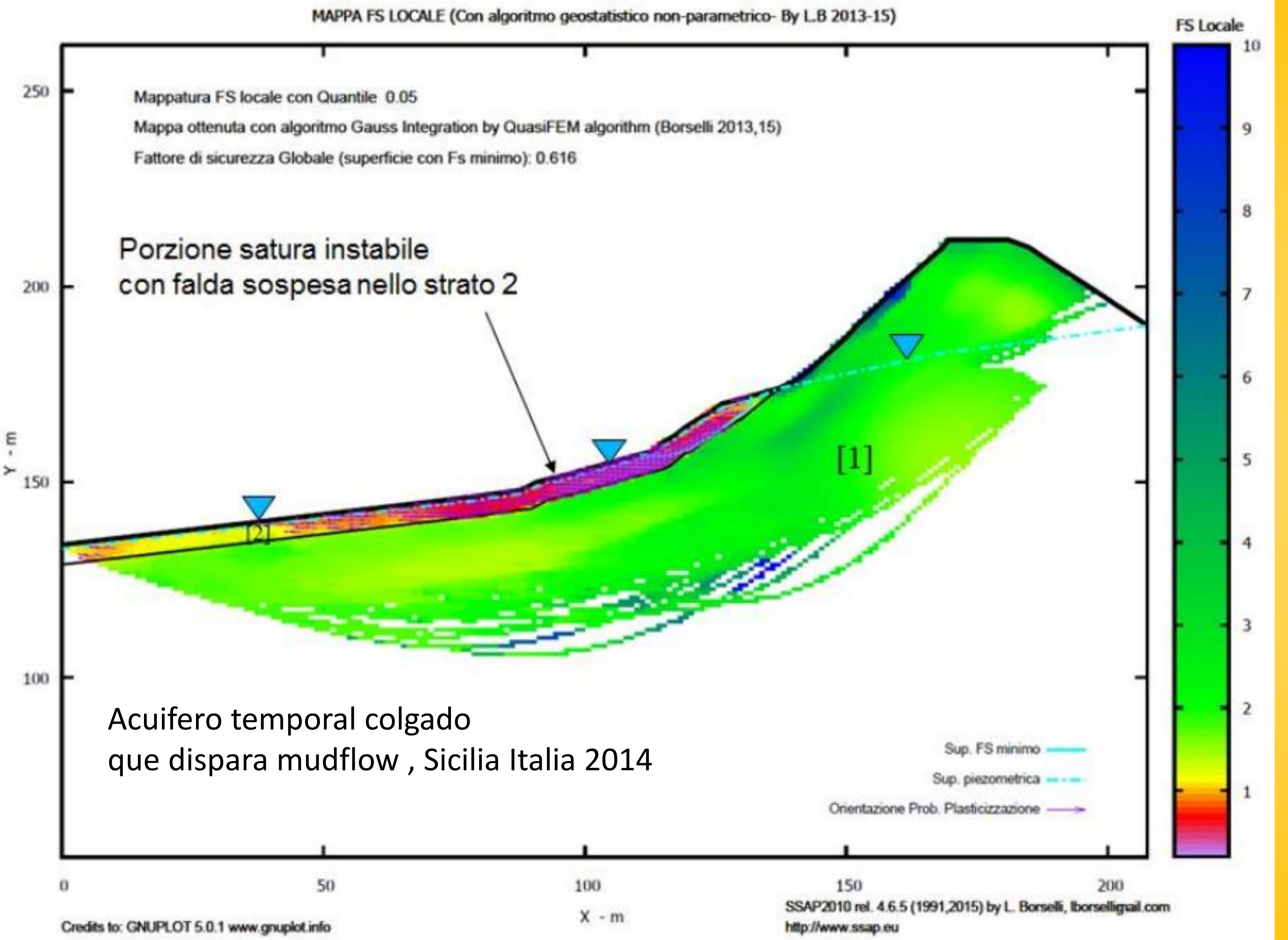

Acuifero temporal colgado
que dispara mudflow , Sicilia Italia 2014

SSAP bibliografía

- BORSELLI L, GRECO L. , PETRI P. 2014. SSAP2010, IL SOFTWARE FREEWARE PER LE VERIFICHE DI STABILITA' ALL'EQUILIBRIO LIMITE (LEM) NEI PENDII NATURALI E ARTIFICIALI, CON METODI RIGOROSI E AVANZATI. Geologi e Territorio , n° 1/2014 - pagg. 22-32 (in italian).
- BORSELLI L, GRECO L. , PETRI P. 2015. VERIFICHE DI STABILITÀ ALL'EQUILIBRIO LIMITE (LEM) NEI PENDII NATURALI E ARTIFICIALI, CON METODI RIGOROSI E AVANZATI PER MEZZO DI SSAP2010 , SOFTWARE DI USO LIBERO (FREEWARE). Informa Geologi. vol. 3 , pag. 27-41 (in italian)
- **BRUNETTI M.T., GUZZETTI F., CARDINALI M., FIORUCCI F. , SANTANGELO M., MANCINELLI P., KOMATSU G. , BORSELLI L., 2014.Analysis of a new geomorphological inventory of landslides in Valles Marineris, Mars, Earth and Planetary Science Letters, Vol. 405: 156-168, ISSN 0012-821X, http://dx.doi.org/10.1016/j.epsl.2014.08.025.**
- **BORSELLI L. 2013. Advanced 2D Slope stability Analysis by LEM by SSAP software: a full freeware tool for teaching and scientific community. IN "ICL Landslide Teaching Tools". KyojiSassa, Bin He, MauriMcSaveney, Osamu Nagai (EDS.). International Consortium on Landslides (ICL). PP. 428. ISBN: 978-4-9903382-2-0.**
- **BORSELLI L.,CAPRA L., SAROCCHI D., De la CRUZ-REYNA S. 2011. Flank collapse scenarios at Volcán de Colima, Mexico: a relative instability analysis. Journal of Volcanology and Geothermal Research. 208:51–65. DOI: http://dx.doi.org/10.1016/j.jvolgeores.2011.08.004**

Mas detallea en el sitio WWW.SSAP.EU

Presentaciones de SSAP descargables desde el sitio WWW.SSAP.EU

- SSAP2010-Slope Stability Analysis Program - Invited seminar CNR-IRPI,Perugia, ITALY, (28 January 2013) (in italiano)

- Evaluación de la estabilidad de taludes complejos en suelo y roca por medio de software SSAP 2010: aplicaciones en Italia y -México (21 March 2013, Mexico ;DF, Sociedad Geologica Mexicana**)(en español)**

- Advanced 2D Slope Stability Analysis by LEM with SSAP software. (PDF tool appendix to.... BORSELLI L. 2013. Advanced 2D Slope stability Analysis by LEM by SSAP software: a full freeware tool for teaching and scientific community. IN "ICL Landslide Teaching Tools". Kyoji Sassa, Bin He, Mauri McSaveney, Osamu Nagai (EDS.). International Consortium on Landslides (ICL). PP. 428. ISBN: 978-4-9903382-2-0) (in english)

- SSAP2010-Slope Stability Analysis Program - Invited seminar, Politecnico di Bari ITALY, (21 January 2014) (in italiano)

Y En YOUTUBE → 6 videos acerca de SSAP de mi canal: Lorenzo Borselli

Gracias por su atención !!!